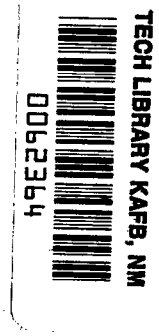

NASA Contractor Report 3742

Preliminary Scramjet Design for Hypersonic Airbreathing Missile Application

Charles H. Carlson

CONTRACT NAS1-15434
NOVEMBER 1983

25th Anniversary
1958-1983

NASA

NASA Contractor Report 3742

Preliminary Scramjet Design for Hypersonic Airbreathing Missile Application

Charles H. Carlson
The Marquardt Company
Van Nuys, California

Prepared for
Langley Research Center
under Contract NAS1-15434

National Aeronautics
and Space Administration

**Scientific and Technical
Information Branch**

1983

TABLE OF CONTENTS

SYMBOLS

A	Area
a	Air speed of sound
C_P	Specific heat
f	Fuel
F	Thrust, Fahrenheit
g	Acceleration due to gravity
h	Heat transfer coefficient, B/sec-in^2 ^oR
H	Enthalpy
I_{SF}	Engine specific impulse
m	Moment
M	Mach number
MS	Margin of Safety
O	Oxidizer
P	Pressure
q	Dynamic pressure
R	Rankine
R_L	Reynolds number based on missile length
S	Length
t	Thickness
T	Temperature

V	Velocity
ρ	Density
ϕ	Fuel equivalence ratio
η_c	Combustion efficiency
η_{KE}	Inlet kinetic energy efficiency
η_N	Nozzle efficiency
τ	Friction coefficient

Subscripts

c	Capture cowl station
i	Internal
NJ	Net Jet
max	Maximum
min	Minimum
r	Recovery
ref	Reference
t	Stagnation
tc	Thermal choke
T	Total
w	Wall
∞	Freestream
0	Conditions behind bow shock, engine inlet entrance station
1	Flow area inlet plane
2	Engine inlet throat station
4	Engine constant area combustor station
6	Engine nozzle exit station

INTRODUCTION

A group at NASA Langley Research Center has been engaged in defining the performance potential and research needs of a hypersonic airbreathing missile concept formulated about an airframe-integrated propulsion system since 1977. This group is now involved in establishing the credibility of their baseline concept as well as an embryonic aerodynamic data base for hypersonic airbreathing missiles (Reference 1). At the request of personnel at the Naval Surface Weapons Center, this group has made a study of a Mach 6 wide-area defense surface-to-air missile concept having a dual-mode scramjet, and adhering to the Navy's vertical box launcher constraints (Reference 2). This system is referred to as a Hypersonic Surface-To-Air Missile (HYSAM) shown in Figure 1. A solid rocket boost to Mach 4 established the takeover condition for the airbreathing propulsion system which then provides the acceleration and cruise performance requirements into the hypersonic speed regime. The Marquardt Company is actively engaged in supplying the efforts associated with the definition of the baseline scramjet propulsion system, including integration, performance, design and structural integrity. The rationale used in defining this propulsion system dates back to the research and development efforts conducted by The Marquardt Company, operating on a contract from the Air Force Aero Propulsion Laboratory. This effort took place during the late 60's-early 70's time period. This particular program established the feasibility of the scramjet as a primary propulsion system for hypersonic missile application.

Analytical and experimental results from direct-connect and freejet engine ground tests were compiled. These tests involved both the hydrogen and the hydrocarbon fueled, dual-mode combustion processes (References 3 and 4). Of particular interest to this program was the freejet engine test demonstrating the hydrocarbon combustion cycle. In concert with this effort an inlet development program (Reference 5) provided inlet characteristics for both the isolated and the missile integrated configuration. This data was obtained using a controlled plenum air flow measuring device. To summarize, this technology was applied to the preliminary HYSAM engine design utilizing design logic, combustor geometry, ignition/sustainer source criteria and the internal parametric component performance. Currently The Marquardt Company is under contract to the NASA Langley Research Center continuing analysis of the scramjet engine components. A report has been released - Reference 6 - which identifies the performance of a scramjet engine in parametric form. This data is unique in that net jet engine performance is readily obtainable for Mach numbers from 4 to 10 ranging from sea level to 100,000 feet for various igniter sources and hydrocarbon fuels.

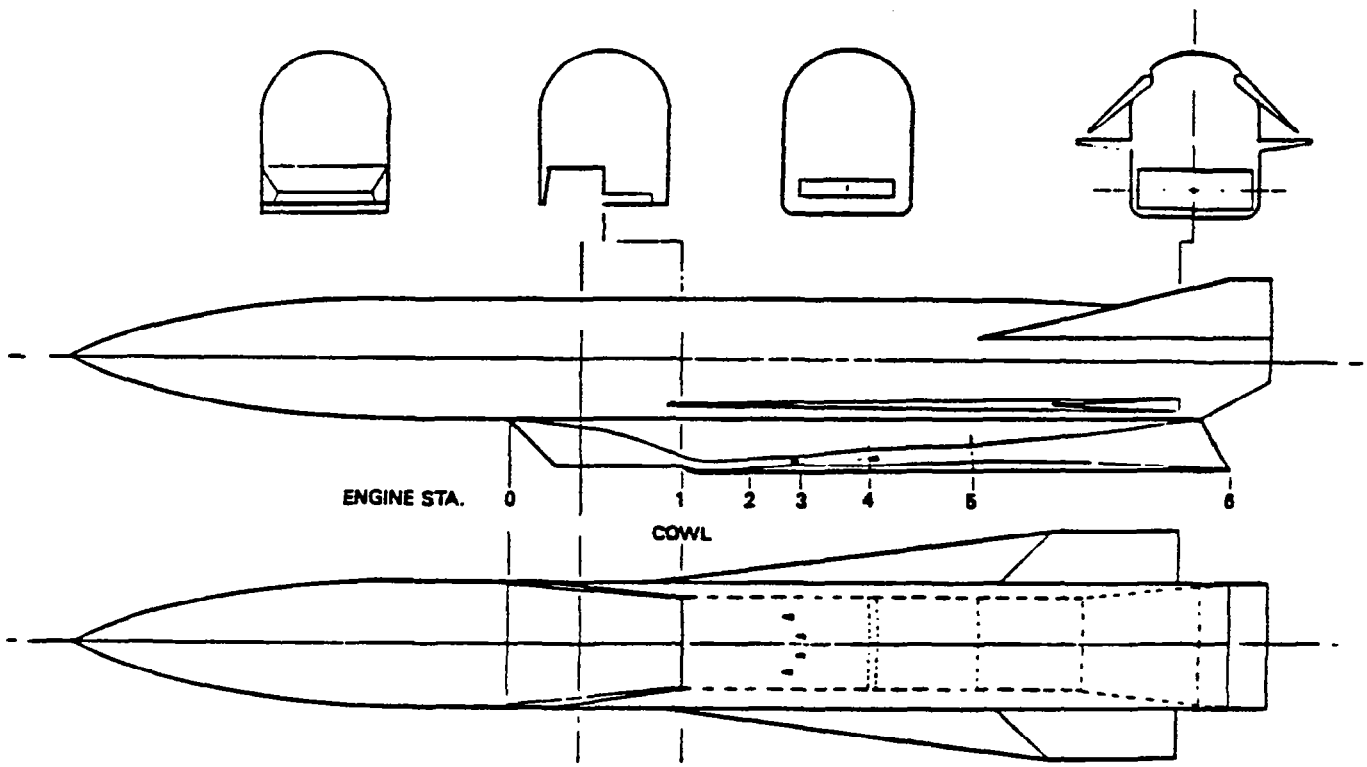

Figure 1. Hypersonic Flight System Concept

Scramjet Propulsion

In addition to the performance analysis a conceptual design study of the scramjet engine was conducted. Definition of the engine was based upon the requirements of accelerating the HYSAM vehicle from Mach 4 at 20,000 feet to Mach 6 at 100,000 feet and the cruise conditions at Mach 6. Takeover at Mach 4 at 20,000 feet prescribed the maximum engine internal design pressure (240 psia) in the diffuser and combustor entrance sector. Partial combustion in this region exhibited gas temperature on the order of 2600 ^{o}F. At the exit of the combustor gas temperatures reached 4700^{o}F. As the freestream Mach number increases the completion of the combustion process for stoichiometric operation gradually approaches the minimum area sector of the engine. At Mach 6.5 the combustion process is completed in the minimum area and the gas temperature reaches 5200 ^{o}F. Throttling the process for cruise operation reduces this temperature to 4750 ^{o}F. These internal environmental conditions were used by the various engineering functions performing design, stress and heat transfer analysis. Material selections for the various engine components were based upon these analyses. This report presents the geometry, design logic, stress, thermal analysis, materials selection and mass properties related towards fulfilling the mission objectives. A two dimensional ramp with laterally contracting sidewalls was selected as the baseline inlet configuration. The engine design was governed by the vehicle geometry, the vertical box launch constraints and the integration of the TMC combustor design logic. A schematic of the internal lines of the previously developed combustor logic and the geometry for this application is shown in Figure 2.

The principal contributors were:

Ken Gable Don Cone'	Design
Bill Roberts Stan Wasserberg	Thermal Protection
Bill Harvey Bob Salcedo	Structure

DEVELOPMENT OF THE SCRAMJET PROPULSION SYSTEM

The development of the scramjet propulsion system for HYSAM is based upon previous Marquardt experience. Technology gained from previous full scale engine development programs established the combustion cycle logic. The data consists of analytical and experimental results from direct connect and freejet engine tests simulating a freestream Mach number of 5.92. Fundamental investigations of bi-liquid pilots and hydrogen-air pilots were conducted during the course of the program. The hydrocarbons used for the tests were JP-7 and Shelldyne-H in liquid form. Liquid chlorine triflouride (CTF) was used as the ignition and piloting source. Equivalence

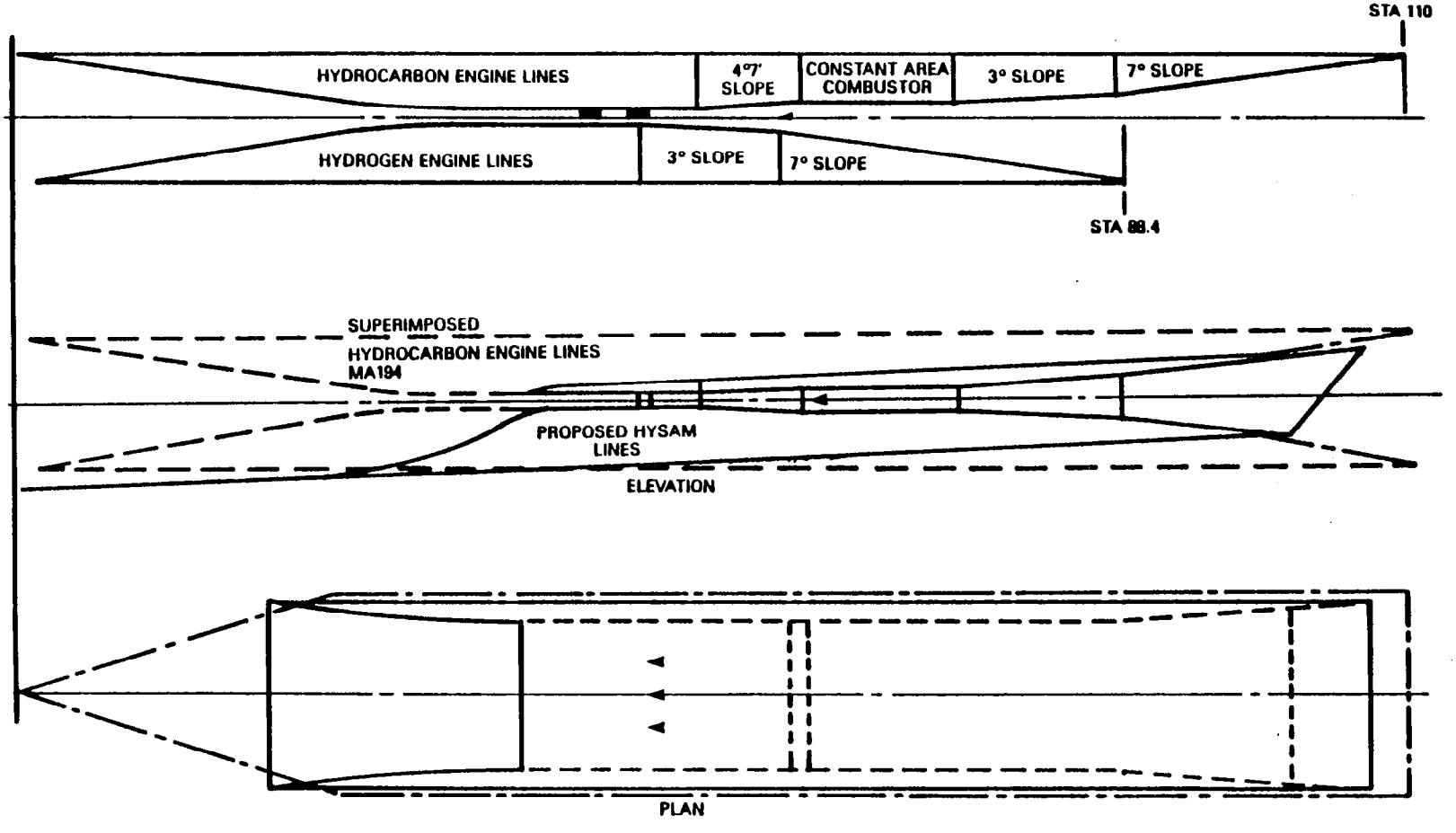

Figure 2. Internal Geometry Comparison of Hydrogen and Hydrocarbon Scramjet Research Engines

ratios (ϕ) from 0.5 to 1.1 and oxidizer-to-fuel ratios (O/F) from 0.05 to 0.7 were investigated. The engine design, fuel-CTF injection configuration and the combustor geometry were based upon the then existing technology developed in previous hydrocarbon investigations. The freejet engine combustor schematic shown in Figure 2, depicts the engine geometry and the location of vertical wedges and the horizontal strut that were designed for both fuel and oxidizer injection. The vertical wedge was used primarily for piloting and fuel injection. The wedge had an included angle of 20 degrees with a triplet in the base for piloting. Fuel injection orifices were also located in the wedge sidewalls. A horizontal strut located at the exit of the divergent combustion chamber was used as an igniter/pilot as well as a low drag flameholder. The strut had an included angle of 16 degrees. Three sets of triplets equally spaced were located in the strut base. There were also 16 equally spaced fuel orifices on each side of the strut sidewalls. The strut provided a means for obtaining good fuel distribution. Flushwall injectors, providing the major portion of the fuel flow, were incorporated in the combustor structure. The engine was tested at total freestream temperatures varying from 2000 ^{o}F to 4000 ^{o}F. Total pressure varied from 660 psia to 1250 psia.

This Scramjet propulsion system is charactertized by two modes of combustion which are: (1) subsonic and (2) supersonic. The estimated performance of the two combustion cycles is nearly the same for the Mach range of interest for the baseline concept (Mach 4 to Mach 6). The subsonic combustion process is similar to the ramjet cycle operating at critical inlet performance conditions. A normal shock is positioned in the inlet diffuser throat area followed by subsonic flow. The combustion cycle is referred to as a thermal choking process. When the Mach number is subsonic, it is assumed that burning will occur in an expanding area and that choking will occur at the same point that burning is complete. It is further assumed that pressure varies linearly with area in this process. In the case where the Mach number is supersonic, an attempt is made to burn all the fuel in a constant area inlet channel. If this is impossible, the fuel-air ratio which thermally chokes the flow is found. The thermal choking fuel-air ratio can be reduced by an arbitrary percentage and the combustion process calculated in the constant area channel for the reduced fuel-air ratio. The remaining fuel is added in an expanding area in either a constant pressure or a constant Mach number process. A combustion efficiency, defined as the fraction of the ideal heat release actually obtained, can be applied to any of these processes. Equilibrium composition is assumed for both air and combustion products through the cycle. The option to freeze the composition of the combustion products at any nozzle station after combustion has occurred exists in the program. After combustion is complete the flow expands isentropically through the nozzle. A nozzle efficiency, defined as the fraction of ideal stream thrust actually obtained, can be applied to the analysis.

A parametric characteristic chart of the supersonic internal cycle process, is shown in Figure 3. The data in the upper left-hand corner represents the results of thermally choking a constant area duct. These variations are based upon the entrance duct Mach number.

The duct entrance Mach number is governed by the inlet contraction ratio, mass flow, pressure recovery, and the freestream entrance Mach number. Inlet contraction ratio (A2/Ac), total pressure recovery (P_{Ttc}/P_{T2}), total temperature ratio (T_{Ttc}/T_T), and static pressure ratio (P_{tc}/P_2), a result of thermal choking, are relationships shown in Figure 3. These functions are based upon an inlet kinetic energy efficiency (η_{KE}) of .975, standard day isothermal conditions, and a combustion efficiency of 90 percent. The fuel used was C.T.F. and RJ-5. As a result of the duct entrance Mach number, the heat release (T_{T4}/T_{Ttc}) theoretically defines the area requirements for the combustion chamber. These relationships are also shown as a function of freestream Mach number. Equivalence ratio for the constant area diffuser duct and the resultant equivalence ratio in the combustor area are shown for combustor area ratios (A4/A2) as they vary with freestream Mach number and contraction ratio complete the geometric sizing relationship. Overall burner recovery is obtained by combining (P_{Ttc}/P_{T2}) and P_{T4}/P_{Ttc}). This parametric study was conducted in the isothermal region for a standard day temperature variation. Slight changes in the combustor geometry occur as a function of the inlet total freestream temperature. The current Marquardt hydrocarbon Scramjet (MA-194 XAB) has an internal geometry relationship A4/A2 of 2.0. Maintaining this sizing relationship would mean that complete combustion at Mach 4 would occur in the divergent region aft of the combustor section.

ENGINE DESIGN

Geometry Definition of the HYSAM Propulsion Configuration

Based on the contour of the HYSAM, which currently incorporates a flat lower surface, a two-dimensional isentropic ramp was selected as the baseline inlet configuration. A 6^o initial ramp followed by $12\text{-}1/2^o$ of isentropic compression for a design (shock-on-cowl) Mach number of 5 was considered optimum for the speed range involved in addition to the assumption that the inlet would operate in a quasi-conical pressure field. In order to maintain the geometry within a given dimension (14.14 inches) laterally contracting sidewalls were incorporated. An angle of 6^o was selected, which can vary depending upon the effects generated by the sidewalls on inlet performance. This design criteria created the following geometric engine dimensional characteristics:

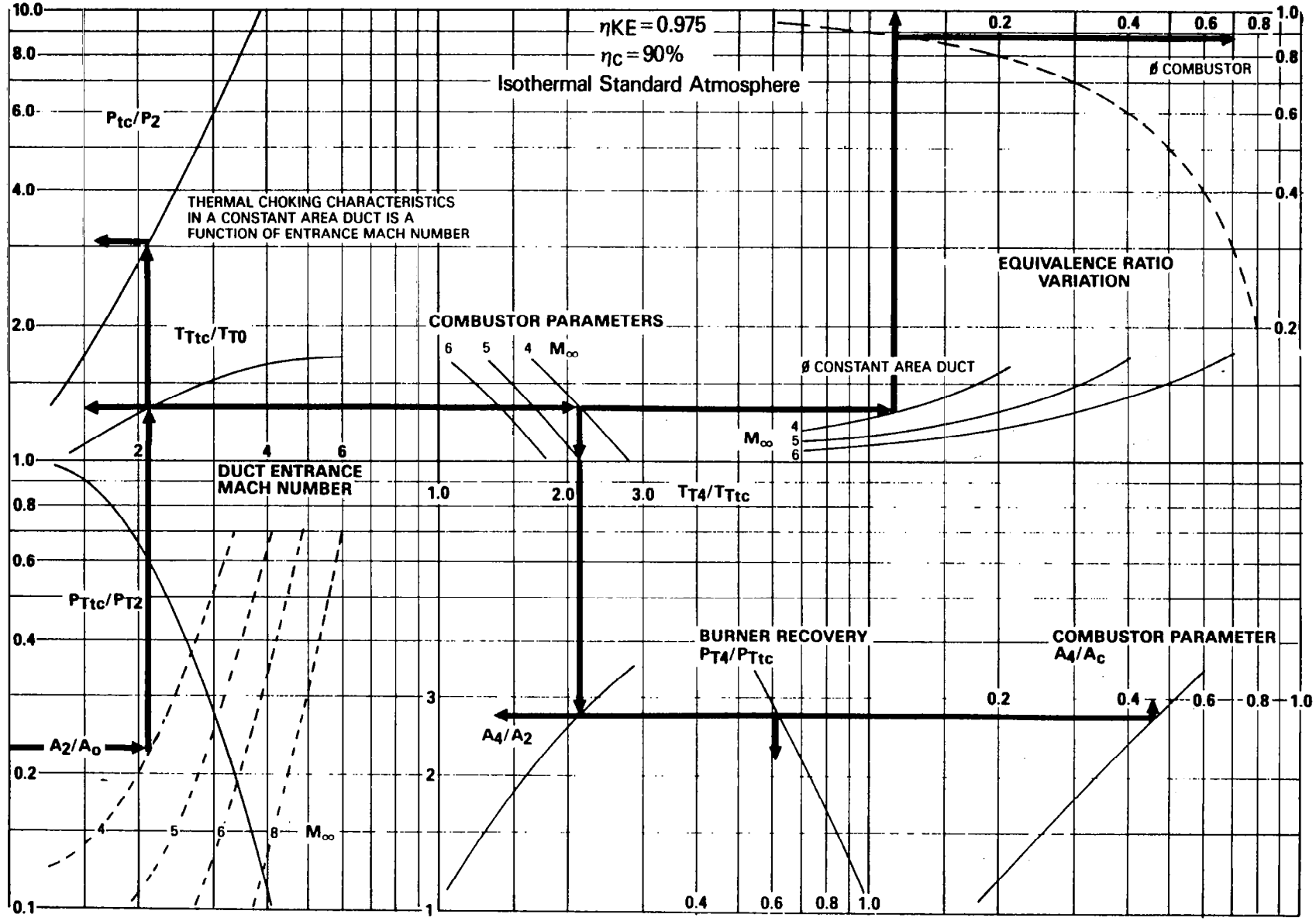

Figure 3. Parametric Internal Component Performance

Projected cowl area - Ac -	76.36 sq. in.
Flow area at inlet plane - A1	16.51 sq. in.
Flow area at inlet throat - A2	12.90 sq. in.
Flow area at combustor - A4	32.25 sq. in.
Flow area at exit plane - A6	85.00 sq. in.
Ac/A1 =	4.62
A1/A2 =	1.28
Ac/A2 =	5.92
A4/A2 =	2.50
A6/A2 =	6.60
A6/Ac =	1.11
Height at inlet plane	1.485 inches
Width at inlet plane	11.12 inches

Capture area was analytically computed based upon the dimensions at the inlet plane and the inlet geometry. Theoretically full capture is obtained at Mach 5.0. At Mach 4 the computed capture area ratio (A_0 /A_c) is 80 percent. These values do not include the sidewall effects which will affect about 30 percent of the inlet flow. An inlet model wind tunnel test program is required in order to establish the inlet characteristics. Figure 4 presents the estimated values of the inlet and the flow field characteristics used for performance analysis. Local Mach number, capture area and pressure field influence is shown as a function of freestream Mach number and angle-of-attack. The basic inlet lines developed for the system are shown in Figure 5.0. Appendix A presents the results of a subsequent study which defined several inlet concepts that would augment the overall system performance.

During the design study communication was established and maintained with manufacturers of combustion chambers that used composite materials. It was through this communication that the shape and method of fabricating a carbon/carbon composite material combustion chamber was formulated. In order to withstand the internal pressures generated in the engine during the takeover and acceleration mode - Mach 4 at 20,000 feet-it became a necessity to prescribe a circular rather than the retangular shape. This criteria affected the inlet diffuser lines and the flow turning requirements. The inlet structure at the cowl lip maintained the rectangular shape from the cowl entrance to a point where the design internal contraction is satisfied. From this station aft to the beginning of the combustor section a transition from rectangular to circular is accomplished. This shape is maintained throughout the combustor and transitions back to the rectangular shape at the nozzle exit.

An internal strut was incorporated in the diffuser for strength purposes. The base of the strut becomes the wedge used to augment the ignition and the combustion sustaining process. The strut terminates in the combustor. During the development phase of the engine a step in the combustor wall would be incorporated if additional flameholding area is required. The trailing edge of the strut incorporates the design features of the wedge that was successfully used during the documentation of the

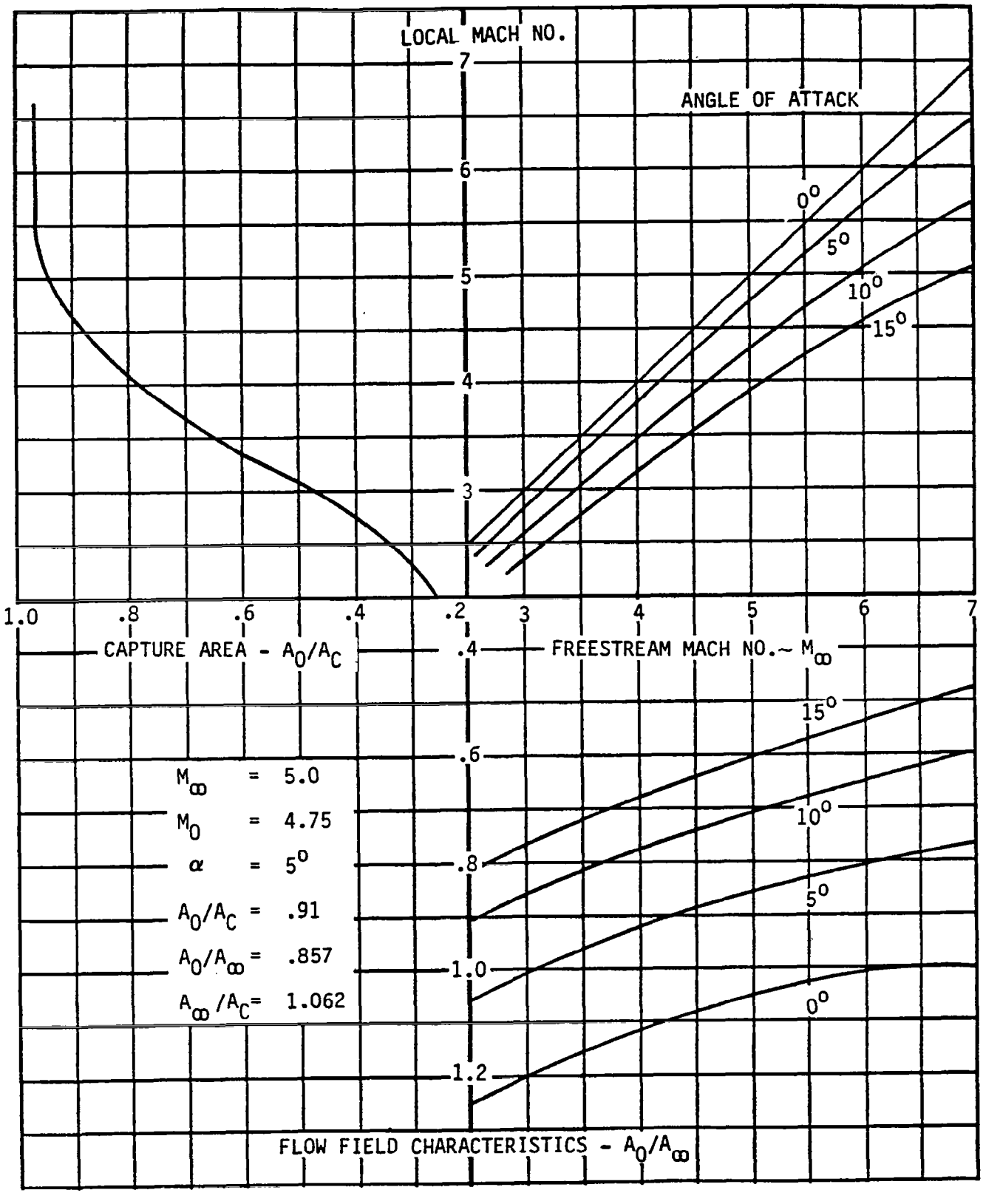

Figure 4. Inlet and Flow Field Characteristics

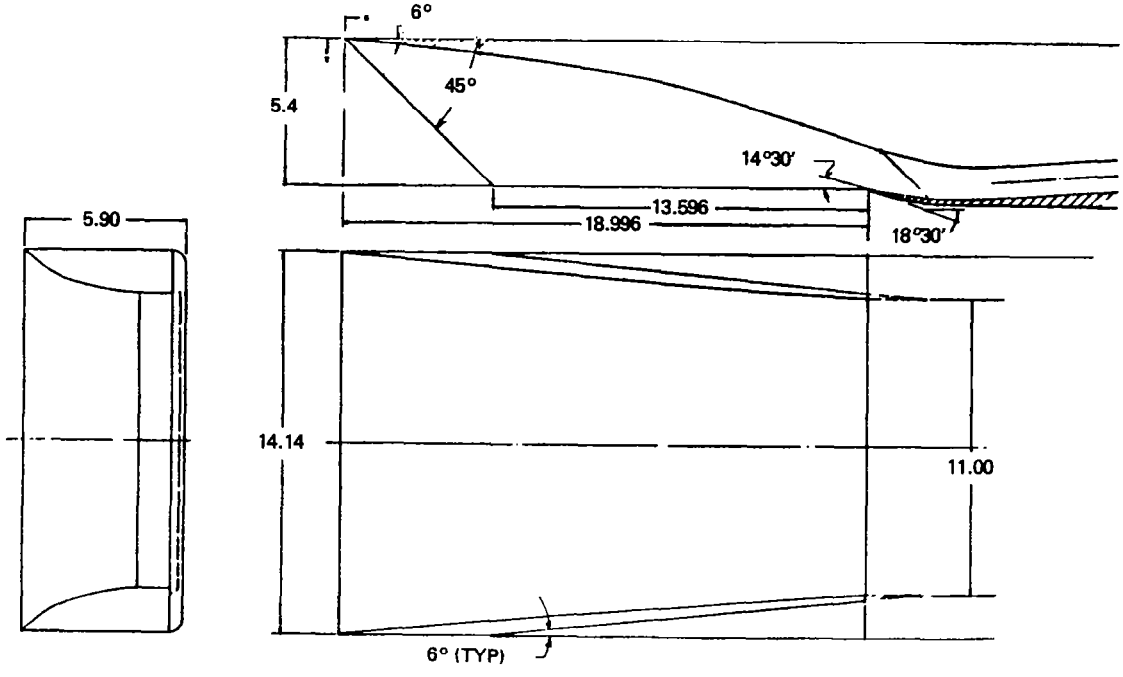

Figure 5. Two-Dimensional Isentropic Ramp Geometry

OTTO fuel II as an ignition/sustaining agent. Primary fuel injection ports are located near the leading edge of the strut. This location is rectangular in shape where good penetration of the fuel into the airstream is anticipated. Vaporization of the fuel is also augmented prior to the ignition process. The OTTO FUEL II is injected forward of the trailing edge of the strut. Finalizing of the combustor geometry, fuel injection location and ignition source will depend upon engine development optimization.

Features that are viable solutions to higher performance include offsetting of the inlet ramp to divert the vehicle boundary layer and/or incorporating a bypass duct inside and aft of the cowl lip. The bypass duct offers several attractive features, such as, increased cowl area, lower cowl drag, boundary layer diversion and improved profiles at the diffuser exit.

The design, the heat transfer analysis, the structural assessment, and the projected fabrication techniques are discussed in the text relative to the described geometry and design constraints.

STRUCTURAL DESIGN

Design objectives of the propulsion system for HYSAM were to refine and describe the engine structure, materials, system components and weight. The earlier conceptual design provided a base from which these objectives could be discussed and studied by all engineering disciplines. Results of the continued study did develop an engine design of lighter weight, material changes, modification of engine structure and a simpler fuel system. This later design is depicted in Figure 6. The engine design now shown reflects these iterations by the engineering disciplines. Although additional analysis and verification of manufacturing techniques, sealing and attachment methods must be further pursued, this engine design does reflect a feasible concept meeting the HYSAM mission requirements.

The HYSAM engine is now designed with a mix of columbium alloys and metal thickness reduced by changes in the bulkheads and webs. The fuel system has been revised to sidewall and flush wall injection. A center web in the duct replaces protruding injectors eliminating individual support, and interface sealing problems of the previous system. A compromise of the inlet diffuser internal lines significantly reduced high stress areas and allowed a reduction in wall thickness and weight. The center web also influenced the structural requirements by reducing the various panel section spans. Although the constant area duct geometry is a transition from rectangular to obround, the fabrication complexity is not severe and the weight gain more than offsets any small manufacturing cost increases. The combustor/exit nozzle section is now a higher strength 3D carbon/carbon component instead of the original 2D concept. This change plus a geometric compromise in the shape also provided thinner wall sections. The reduced thickness also allowed added depth/volume between the inner structure and the outer shell of the engine. The added depth allows sufficient volume for insulation between the inner and outer structure. Insulation

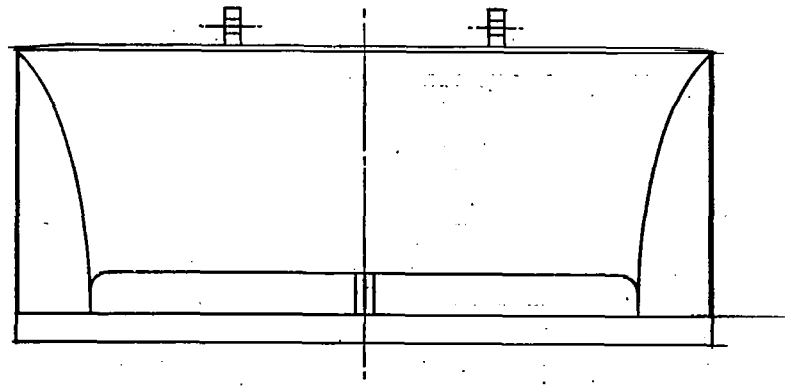

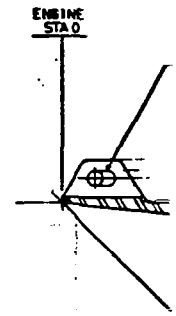
ENGINE
STA 0

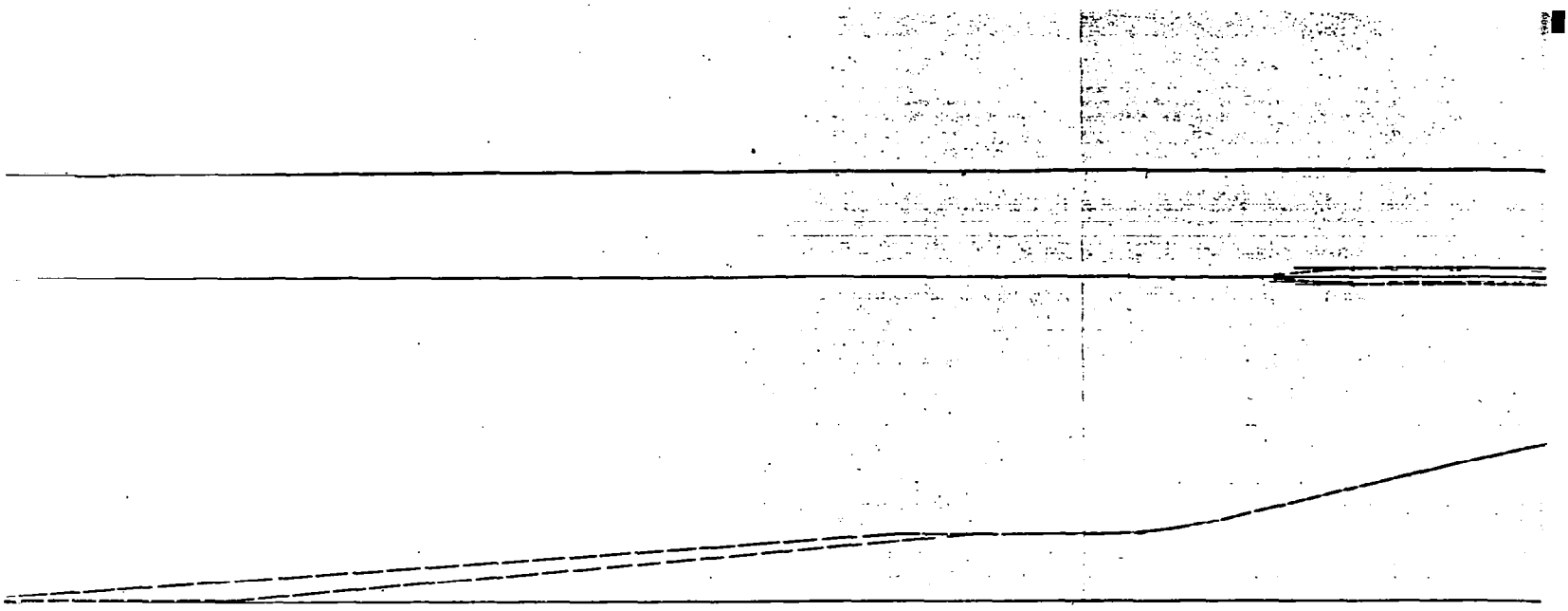

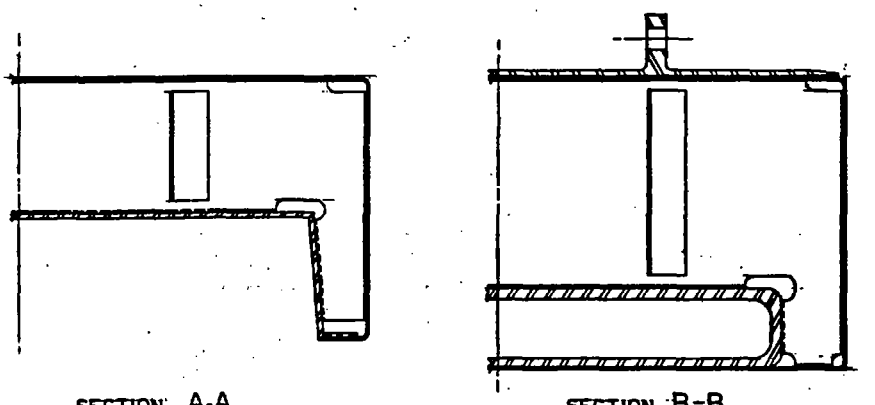
SECTION A-A
STA 1612
SECTION B-B
STA 23.85

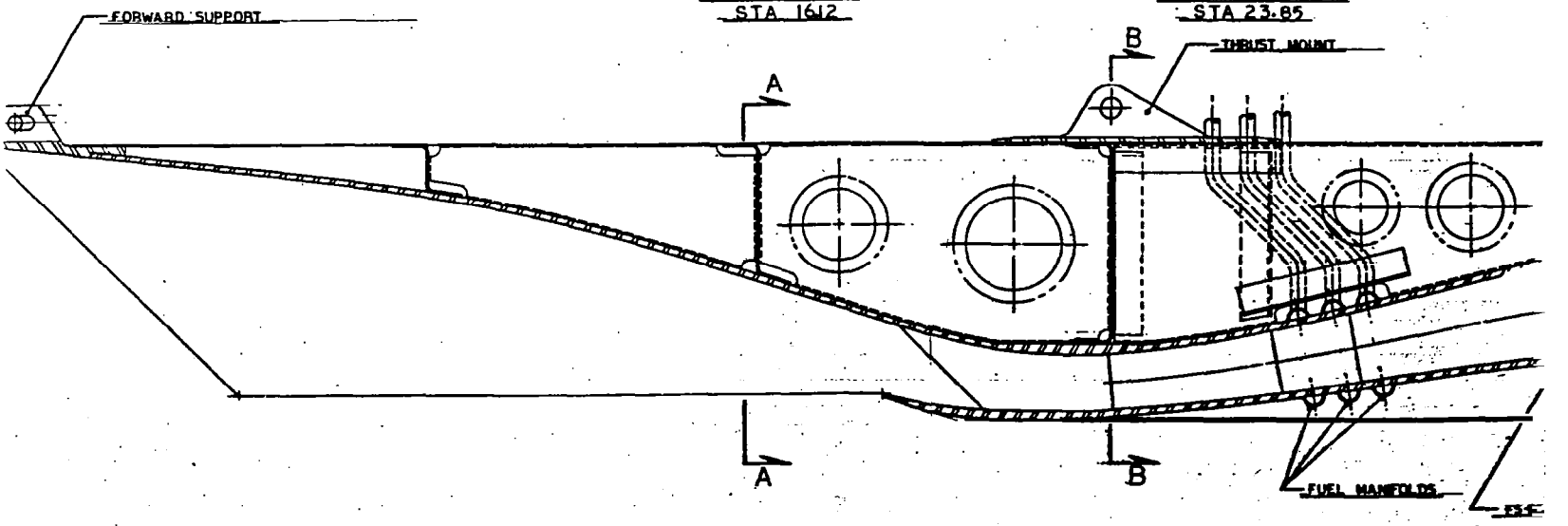
FORWARD SUPPORT
A
B
THRUST MOUNT
FUEL MANIFOLDS
FS 1

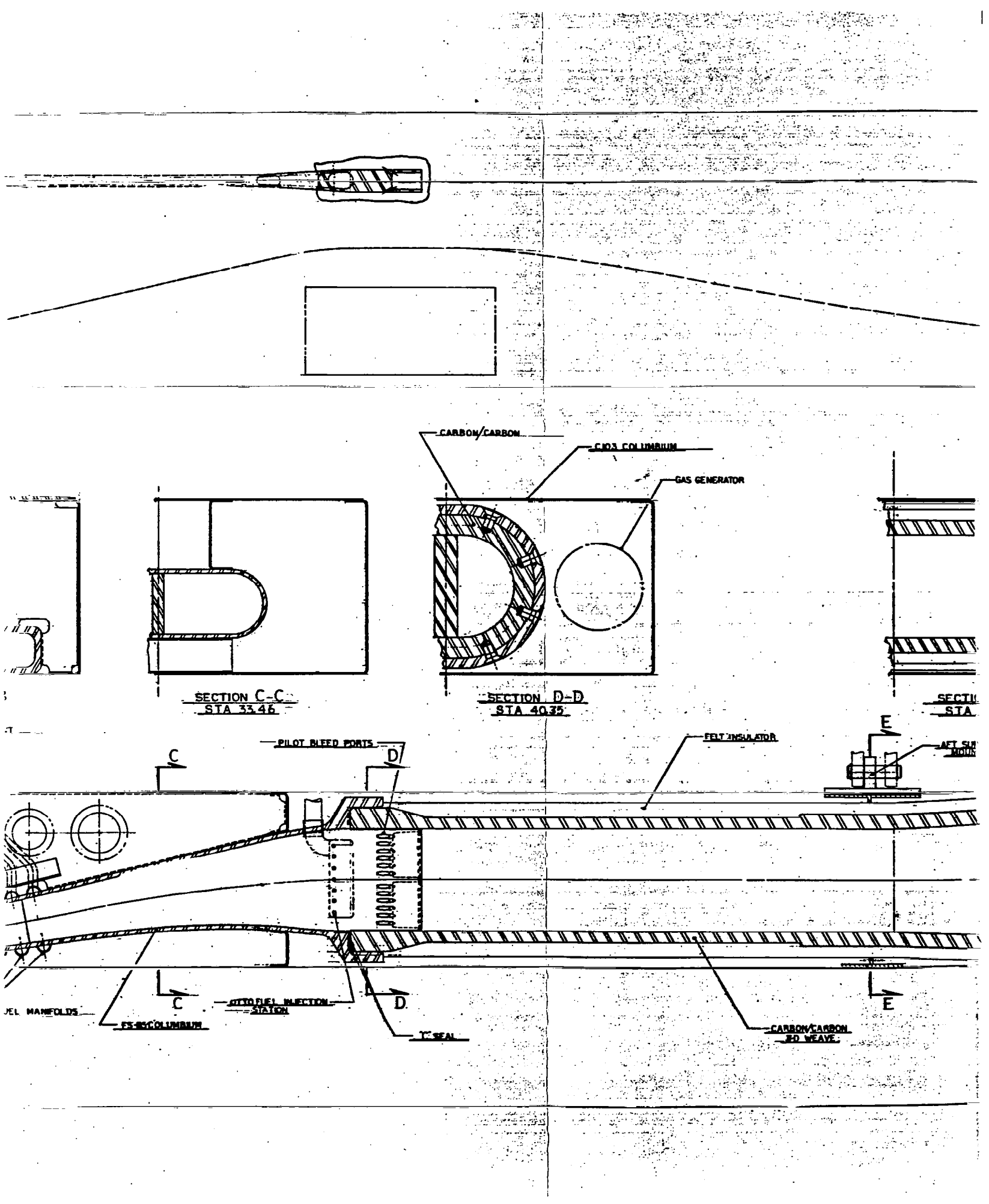
CARBON/CARBON
C103 COLUMBIUM
GAS GENERATOR
SECTION C-C
STA 33.46
SECTION D-D
STA 40.35
SECTI
STA
PILOT BLEED PORTS
C
D
FELT INSULATOR
E
AFT SU
MOUN
JEL MANIFOLDS
FS-85 COLUMBIUM
OTTO FUEL INJECTION
STATION
C
D
E
SEAL
CARBON/CARBON
3D WEAVE

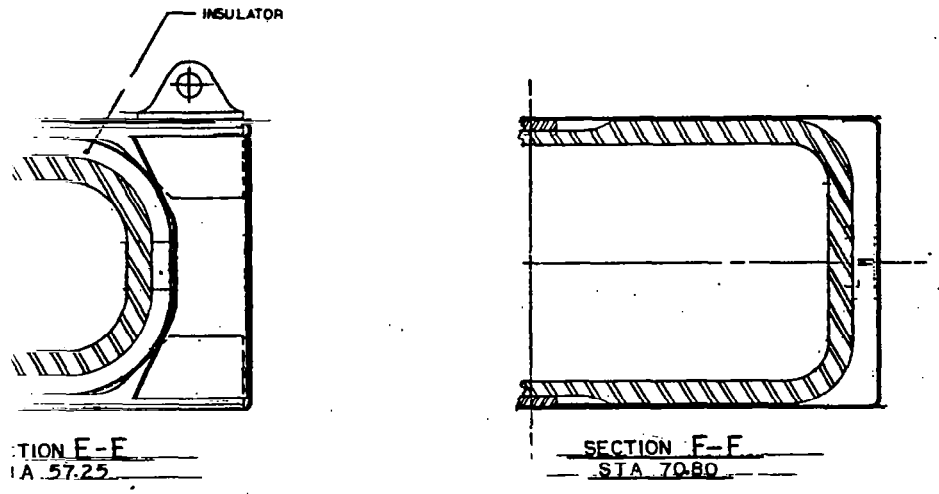

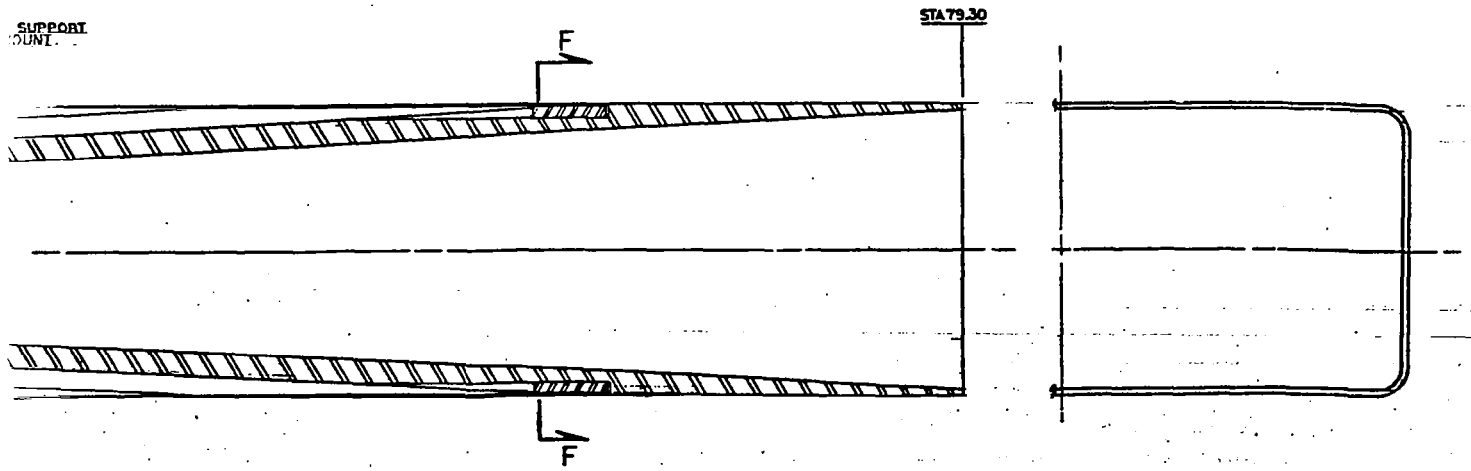

SCRAMJET PROPULSION SYSTEM
NASAN APPLICATION
1-10422 C

Figure 6

surrounding the carbon/carbon structure was reviewed and instead of the zirconium oxide used on the original concept, it is now a carbon felt. A monocoque shell structure surrounds the internal ducting of the inlet and carbon/carbon combustor/exit nozzle section. Material selected for this structure is now columbium alloy C-103. Engine attachment to the vehicle is shown at three axial locations. The forward and aft support lugs allow for thermal growth differences between the engine components and the vehicle. The main center support lugs transfer the engine thrust loads to the vehicle.

Each section of the engine is discussed in more detail as follows:

Inlet Section

The two dimensional inlet section consists of the aerodynamic compression ramp, contracting sidewalls, a cowl lip and the internal duct to the throat. Axially this section is from engine station 0.00 aft to station 23.85. Figure 6 (L10422C) defines engine stations. Section views A-A and B-B show the inlet cross-section geometry with structural webs and frames.

Structural analysis was performed to determine the lightest columbium alloys for structure to reduce weight wherever possible. Two alloys FS85 and C103 were assumed for this task. The FS85 alloy is a higher strength alloy than the C103 but C103 is a lighter material. The most severe loading condition and thermal environment was determined at M_∞ = 4.0 at 20,000 feet. Material properties were compared and it was decided that the main load carrying structure and leading edge components were lightest with the FS85 alloy and that shear panels would be lighter using the C103 material. The end result of these design iterations did provide decreased material thickness and a lighter weight section than the original preliminary design. The recommended thickness of various engine structural components are discussed in the stress analysis section of this report. Future iterations are expected to refine these conclusions and reduce weight by using more of the C103 alloy.

Protective oxidation coatings are considered a requirement for the inlet section leading edges, however since the flight time duration is relatively short, this may not be necessary. Future evaluation and testing of specimens at predicted environments for flight would provide confirming data. Newer columbium alloys are more resistant to oxidation at higher service temperatures than the alloys assumed herein. Review of other candidate materials would be a requirement for use in a final design. For any freejet ground tests where repeated cycles occur, the oxidation protective coatings may be a requirement if the FS85 and C103 materials are used.

Fabrication of the inlet section would be a weldment consisting of sheet stock and plate that is machined. From the lip aft to station 23.85 corner radii develop to enter the fuel injection/constant area duct section. The reference Figure 6 depicts the inlet and constant area duct as one unit of the engine. However, the sections are described separately for definition of the engine geometry and structure. Welded

interfaces joining these two sections make the forward portion of the engine. The structural webs and frames with the outer shell closure complete this entire forward section.

Fuel Injection/Constant Area Duct Section

The constant area duct section as previously stated is a continuation of the inlet duct aft of station 23.85 and extends aft to station 42.20. This portion of the duct transforms the two dimensional inlet geometry into an oval shape. From station 23.85 aft, a center duct divider extends to station 42.20 into the carbon/carbon combustor section. The duct section also includes all fuel injection systems and has been designed to be the engine main thrust reaction structure for axial load transfer to the vehicle. The contoured duct material is the FS85 alloy. The webs, frames and outer shell have been designed with the C103 alloy.

Flush wall fuel injection is shown at the top and bottom walls of the duct. Fuel manifolds are fixed to these walls and supply lines routed to the upper cavity into the vehicle. An OTTO fuel injection system is provided for at the aft end of the duct divider. A manifold in the divider and injection ports on each side provide OTTO fuel injection into the duct. The fuel injection systems now eliminate previous problems of sealing and regenerative cooled struts shown in the earlier engine designs.

The main differences of the section over the previous designs are the changes in geometry and the use of columbium alloys further aft in the duct, moving the interface of the carbon/carbon section further aft. This interface joint is now at station 40.35 shown at section D-D of the referenced engine drawing. Attachment of the combustor/exit nozzle was also redesigned to a more conventional method and reduced in size. The carbon/carbon combustor is captured by the columbium flange lip at the end of the inlet constant area duct section.

As stated previously, the fuel injection/constant area duct section is joined with the inlet to become one integral unit of the engine. A forward vehicle attachment mount on the inlet leading edge just aft of Station 0 and a thrust mount at station 23.85 combined with the monocoque shell complete the inlet assembly.

Combustor/Exit Nozzle Section

The combustor/exit nozzle section extends aft from the interface station 40.35 to engine station 79.30. Geometrically, it begins as obround and transitions to a rectangular section with radiused corners. The carbon/carbon chamber in this concept is fabricated from a 3D woven matrix and formed over a mandrel. Earlier designs were of a 2D weave, but revision of cross-section shape and improved fabrication methods by the manufacture (Fiber Materials Incorporated) allowed changing to the 3D weave matrix of this design. This change provided higher strength material and, therefore, thinner wall and less weight. Another benefit was an increase in depth/volume between the combustor and outer shell providing added space for an insulation blanket.

Because the carbon/carbon material has high thermal conductivity, it is necessary to protect the monocoque outer shell structure with a thermal barrier. Heat transfer analyses predicted extremely high temperatures at the outer wall of the carbon/carbon combustor (see section on heat transfer analysis). Several insulation materials were reviewed for use on the engine during the design. The first choice of zirconium oxide was dropped after further review showed physical and mechanical properties (bonding, shrinkage and conductivity) were unfavorable. Other refractory fiber materials were reviewed for their use to find a more compatible material. The choice now is either a graphite felt or a carbon felt wrapped around the combustor and stitched with the same material yarn. Carbon felt has been assumed for the design shown. Figure 7 shows four felts that were reviewed. The white samples are refractory fiber materials made from blends of alumina silica but are limited to 3000°F. These materials are supplied as a moldable moist felt and during drying become rigid. The black samples are graphite felt and carbon felt. The carbon felt has lower conductivity, a much higher temperature range and therefore was the choice for the present design. Heat transfer analysis confirms this choice. If necessary, the possibility exists that the carbon felt could be wrapped with the alumina silica felt, but at this time, the carbon felt is adequate to protect the columbium outer shell.

The combustor/exit nozzle attaches to the inlet ducting as a shear joint using columbium shear bolts. A tentative seal face using "c" seals has been shown but further investigation and design effort are recommended to harden this interface concept. At the aft end, the monocoque shell slides on the carbon/carbon nozzle to allow for thermal growth differences. The shell and combustor are independent sections and, as described in the structural analysis, are each simply supported beams with deflections near the same. This coincidence eliminates the necessity of added supports for the shell and simplified the design. Heat transfer from direct contact of structural supports was a concern on the earlier designs since it meant that thermal isolation materials that carry load would be required and conductivitity to the outer shell was excessive for all materials reviewed.

The present combustor/exit nozzle design now is lighter in weight and requires no supports for the shell between the forward and aft end.

The three-dimensional carbon/carbon section, because of its shape, represents a development program for the industry source of such materials. FMI was responsive to TMC's inquiries and recommended a plan to develop four units. Time to develop, produce and delivery the four items was approximately one year. This time period would be after a firm design of the engine combustor/exit nozzle has been accomplished.

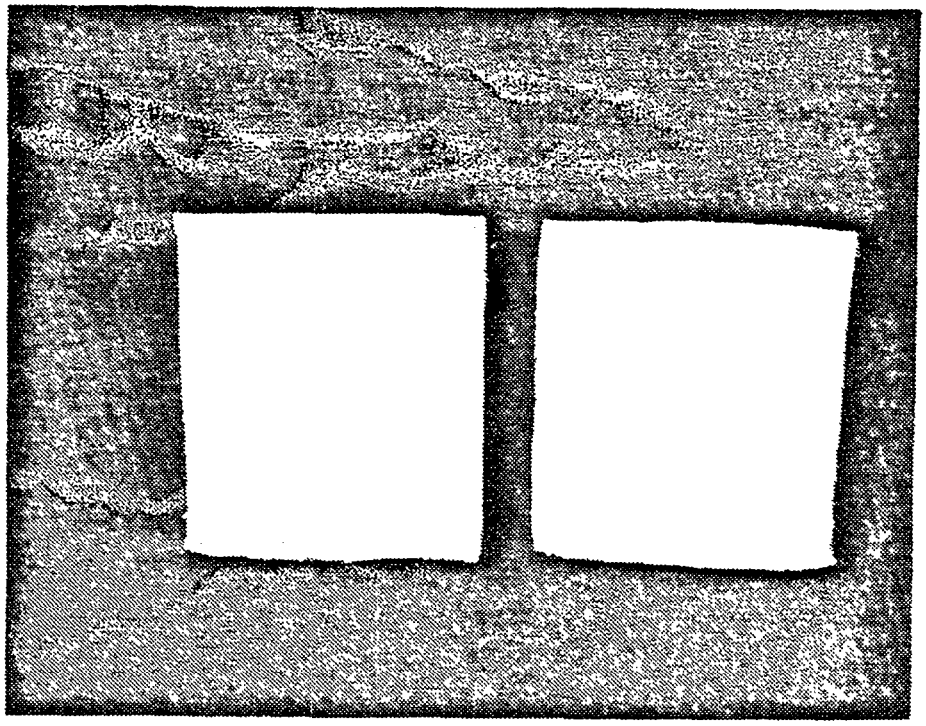

Alumina Silica Felts

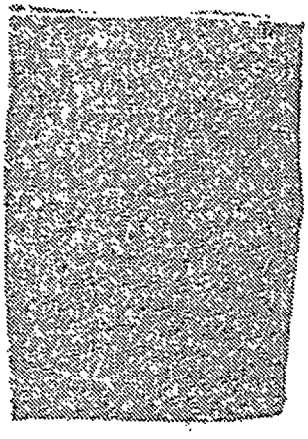

Graphite Felt

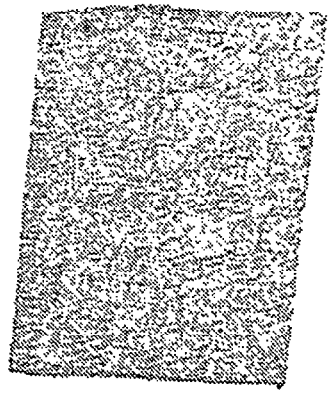

Carbon Felt

Figure 7. Insulation Materials

The monocoque shell enclosing the combustor has, at station 57.25, the rear support for the engine to vehicle mount. It has been designed to provide thermal growth of the engine components between the thrust mount at station 23.85 and to provide thermal growth differences of the engine and vehicle.

The shell enclosure is also designed with the C103 alloy to be compatible with materials of the forward inlet duct section. However, heat transfer analysis show that the outer shell does not exceed 1500°F and the possibility of alternate materials for this section and those aft of the inlet exists. Several factors influence the choice of the columbium alloy but other material choices should not be ruled out until a final design is accomplished.

Design Summary

The HYSAM engine preliminary design derived at after several iterations has accomplished a reasonable concept. The design should now be addressed in detail and a firm concept made.

It has been the intent to provide an engine that will meet the HYSAM requirements, and be designed with state of the art materials and technology. From this preliminary design, a final engine concept may be derived. The engine weight has been estimated as approximately seven percent above the goal of 125-130 pounds. Further, definitive detail design will be required to establish a final engine concept and actual weight. The structural weight estimated herein did not consider system components which would be additive. However, this study did produce a reasonable design that is very close to the weight requirement for the HYSAM vehicle.

THERMAL ANALYSIS

Thermal analysis of the HYSAM scramjet has produced a thermally viable configuration. The engine basically consists of a three-dimensional carbon/carbon (c/c) combustor/nozzle liner secured to an FS-85 columbium inlet. The c/c liner is sheathed with carbon felt insulation to thermally protect the FS-85 engine structure and skin. Fuel is injected into the engine air flow about midway between the inlet cowl and the forward end of the c/c liner. The OTTO II ignition/sustaining agent is injected from a strut near the leading edge of the c/c liner. The results of the thermal analysis of these components are discussed in the following paragraphs. In addition, a fuel regeneratively cooled combustor and strut were thermally analyzed but not included in the final design. The results of this analysis are also included.

Analytical Methods

A passive thermal protection system is utilized in the engine. Consequently, the thermal response of the system is transient in nature, with varying flight conditions. The boundary conditions for the subject analyses were computed along a preliminary design trajectory. With this trajectory, the engine accelerated, with a combustion equivalence ratio, ϕ, of unity, from a flight Mach number of four at 20,000 feet of altitude to a Mach number of six at 100,000 feet in 160 seconds. Then, the ϕ was reduced to 0.7 and the engine cruised at the latter flight conditions for 180 seconds. After this 340 seconds of thermal exposure, the design mission was considered terminated.

The external aerodynamic heating heat transfer coefficient was computed using the Eckert Reference Temperature Method for a flat plate. Several flat plate methods as well as the Bartz method were investigated for use in computing the internal heat transfer coefficient. All methods resulted in the combustor liner hot wall temperature being within 200°F of combustion gas total temperature because of the external insulation around the c/c liner. Under these conditions, accuracy of the internal coefficient becomes much less important than in regeneratively cooled, metal walled, Scramjet engines. In light of this, the Bartz method was used.

To perform the transient analyses, thermal models were created for the various engine components and temperature solutions were found using the Marquardt Thermal Analyzer Program. Two-dimensional thermal models were used for the inlet and the c/c joint region. One-dimensional models were used elsewhere in the c/c liner.

Combustor/Nozzle C/C Liner Analysis

The thermal analyses of the combustor/nozzle c/c liner, the felt insulator and the columbium engine structural skins were conducted at selected axial locations along the liner. Temperature solutions were found for the lower, 6 o'clock region and the upper 12 o'clock region. This was because the lower skin is exposed to aerodynamic heating and overboard cooling by radiation. The 12 o'clock skin is not exposed to aerodynamic heating but does radiate to an assumed identical interface skin which is part of the missile body.

The temperature results of the analyses conducted at station 4 are shown in Figures 8 and 9 for the 6 and 12 o'clock locations, respectively. Maximum c/c inner surface temperature (node 5) reached about 4500° at the end of the 160 second acceleration period and cooled to about 4200°F by the end of the cruise period of the trajectory. The low thermal conductivity of the carbon felt insulation caused a large temperature drop (up to about 3000°F) between the c/c liner and the external skins. The external skin at 6 o'clock heated more rapidly than the 12 o'clock skin due to aerodynamic heating during acceleration. Both skins reached a maximum of about 1500 ° F. The felt insulation and the heat capacity of the missile interface skin combined to maintain the 12 o'clock engine skin at about the 1500° F level.

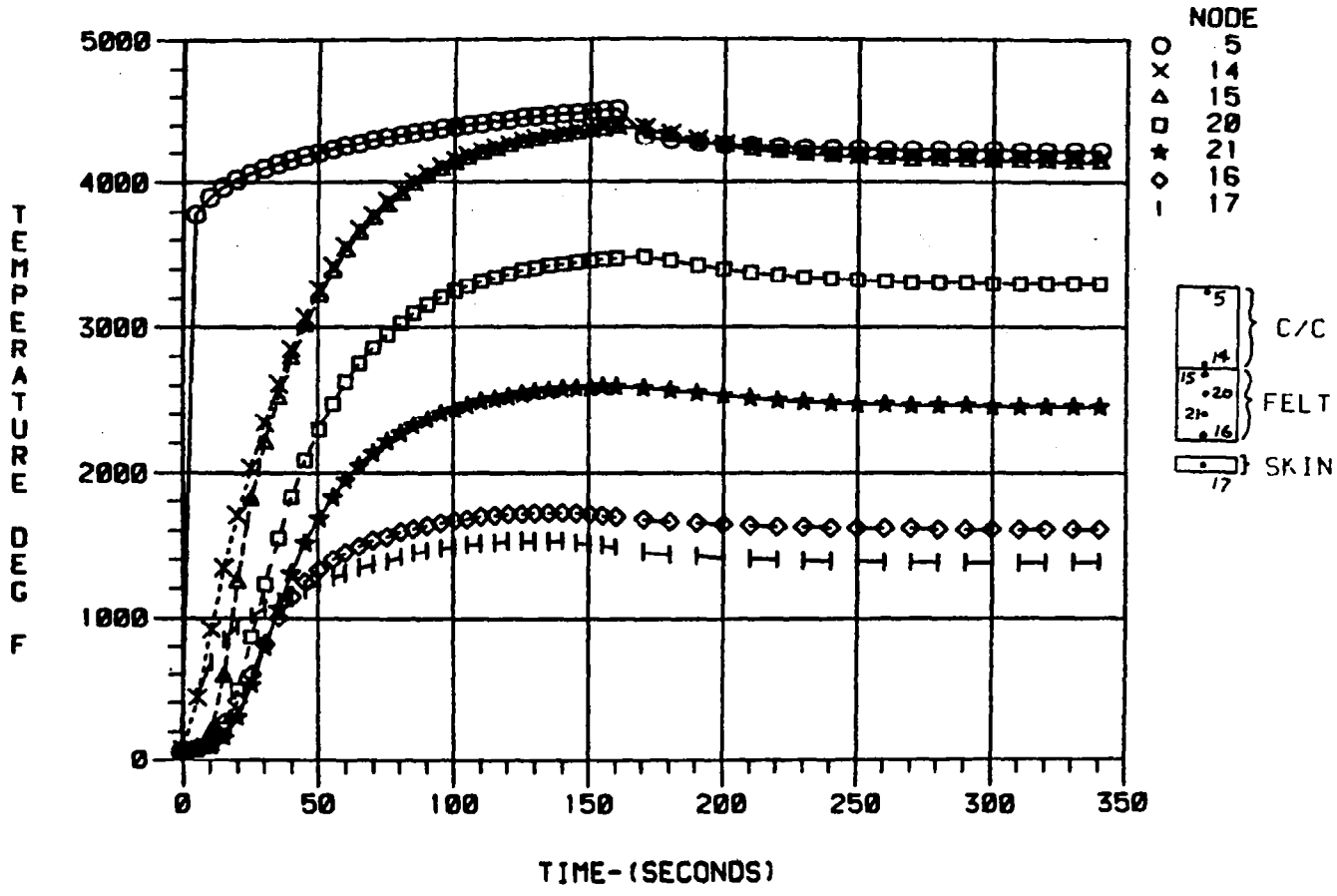

Figure 8. HYSAM Scramjet Combustor Material Temperatures
6 O'Clock Location, Carbon Felt Insulation
Temperature vs Time

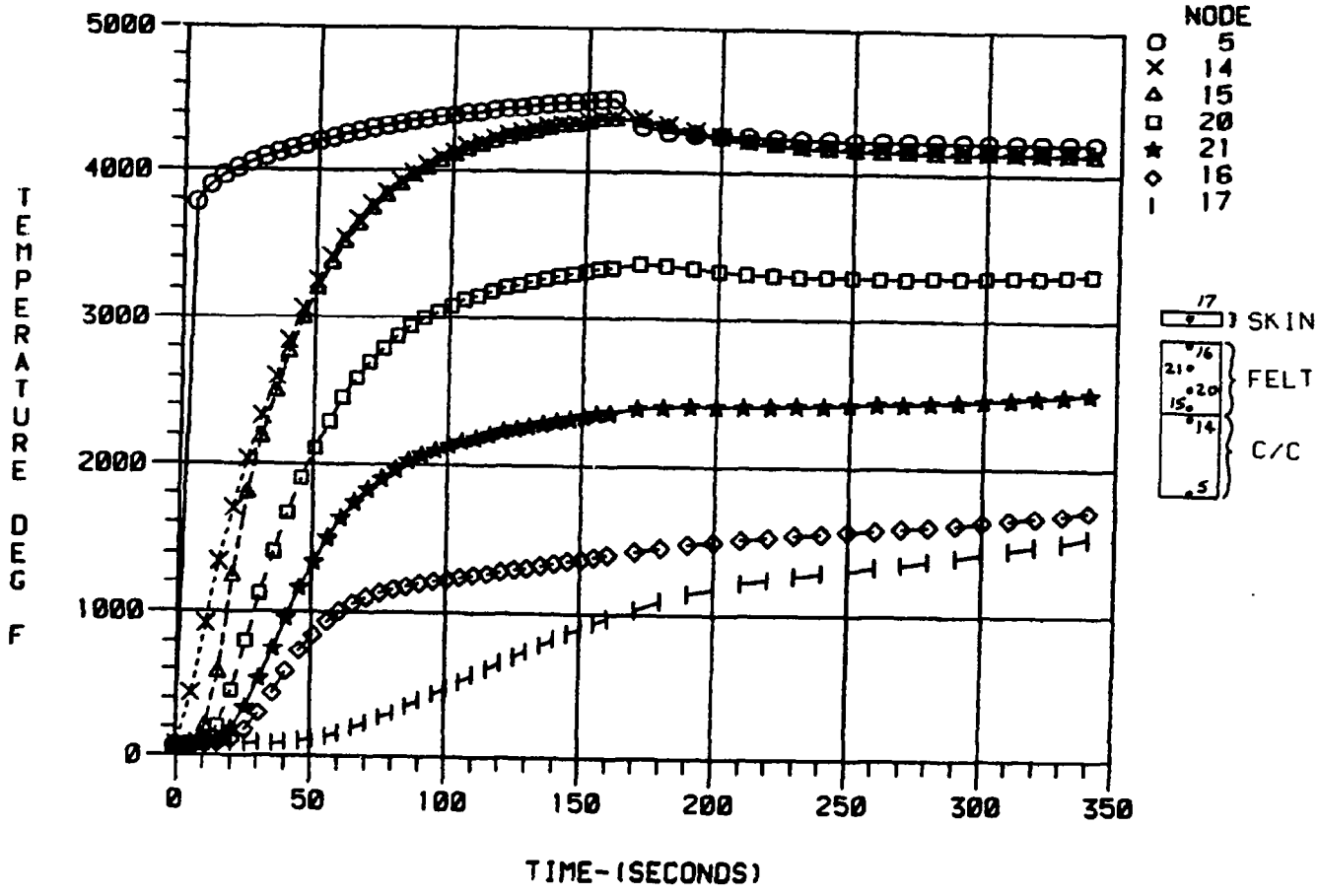

Figure 9. HYSAM Scramjet Combustor Material Temperatures
12 O'Clock Location, Carbon Felt Insulation
Temperature vs Time

Temperature values from analyses at other axial locations along the liner and the inlet (described below) were utilized to plot axial temperature distributions of the inlet duct, c/c liner, felt insulation and skins. The axial temperature distributions are shown in Figures 10 and 11 for the 6 and 12 o'clock locations, respectively. Figure 11 shows the axial temperatures at 12 o'clock at the end of the trajectory when the internal skin is the hottest. The inlet cowl reached about 2300°F at the leading edge and the duct temperature closely followed the internal recovery temperature at about 2200°F. The radiant heating of the skins by the hotter duct is apparent in both locations. Temperatures at the nozzle exit reduced drastically due to external aerodynamic cooling and radiation. The OTTO II strut injector will operate about 100°F hotter than the duct, or about 2500°F. The base of the strut will tend to run hotter unless insulation or fuel cooling are utilized. This strut was not analyzed in detail.

Inlet Analysis

The structural design point of the inlet was at a flight Mach number of four at an altitude of 20,000 feet. Thermal analysis of the inlet component provided the axial temperature distributions shown in Figure 12. The Eckert flat plate reference temperature method was used for duct and cowl heating. These temperatures were used in structural analysis of the FS-85 inlet. Inlet air stagnation was assumed at the compression ramp leading edge, which is conservative. At cruise Mach number, inlet temperatures were higher reaching 2300°F internally as shown in Figure 10. This dictated the inlet material selection.

Carbon/Columbium Joint Analysis

The temperature of the joint where the c/c liner is joined to the inlet duct was of major concern because of temperature limitations on the duct. Locating the OTTO fuel injector base downstream from this joint, provided enough axial distance to sufficiently cool the c/c liner with inlet air as shown in Figure 13. Downstream from the idealized, worst case, flame front, the c/c liner was over 4000°F. As a result of the above cooling, and radiation to the cooler skins, the joint temperature was about 2250°F. This is acceptable with the FS-85 material.

Fuel Cooled Strut Analysis

A regeneratively cooled fuel injector strut was analyzed and the results are shown in Figure 14. By taking the fuel cooling approach, a relatively cold strut body would be provided which would aid mounting and sealing in the hot c/c liner. Also, fuel temperatures could be maintained below the coking level prior to injection. As shown, strut cold wall temperatures were about 650°F in the passages. This required six passes of fuel coolant along the length of the strut. Fuel entered the strut at 70°F and was heated to 300°F by convection. The maximum strut hot side temperature was about 900°F. These temperatures resulted during the cruise condition at a ϕ of 0.7 with all 0.3 lb/sec of engine fuel cooling the injector. This configuration was not utilized in the engine design but the cooling techniques analyzed here might prove useful in the actual strut.

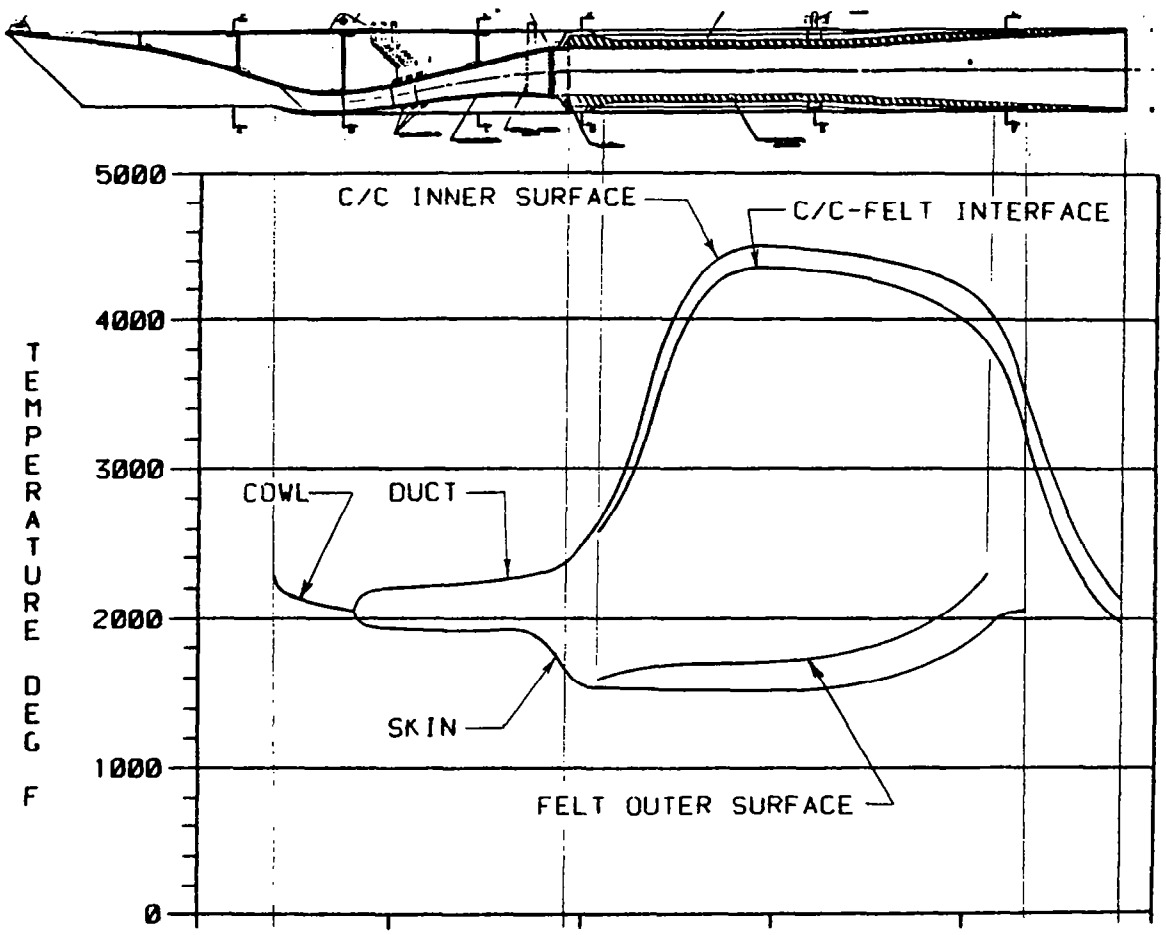

Figure 10. HYSAM Engine Material Temperatures, 6 O'Clock Location

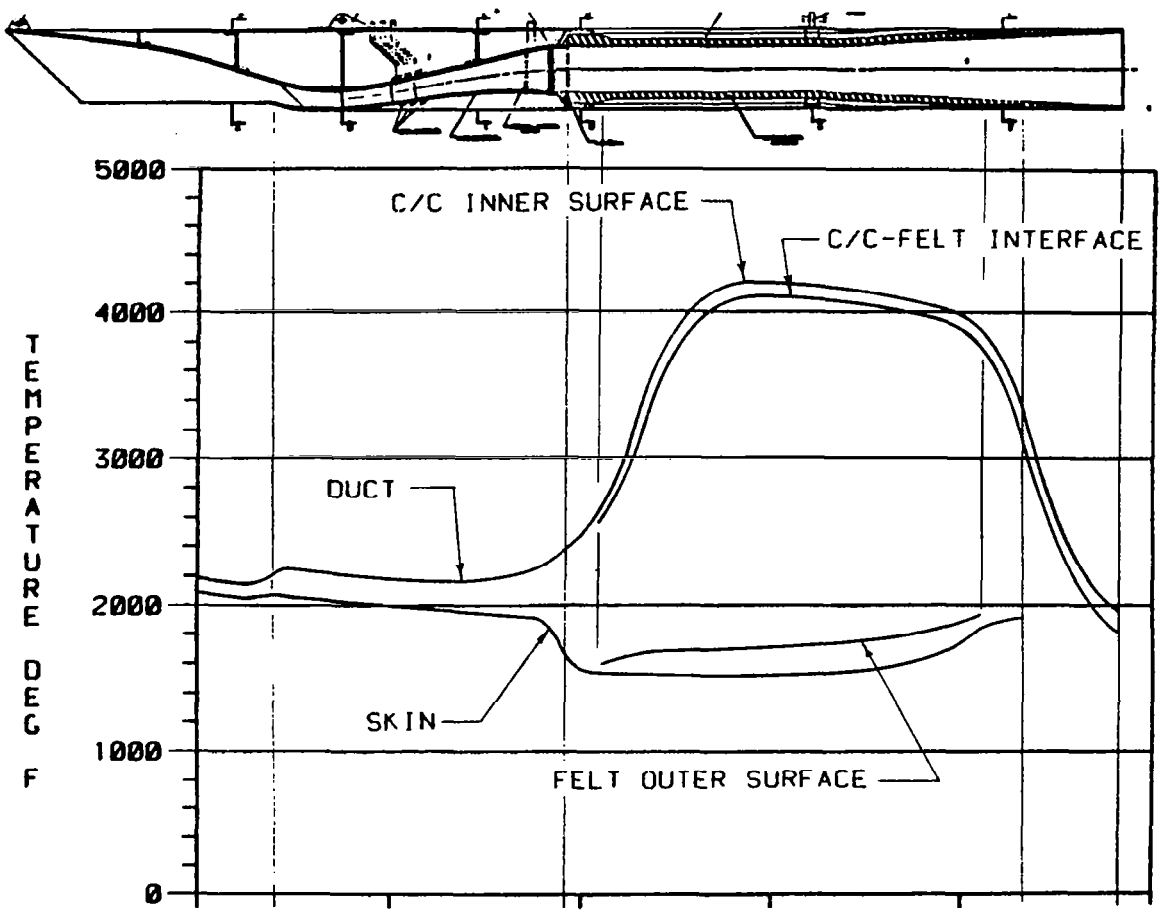

Figure 11. HYSAM Engine Material Temperatures, 12 O'Clock Location

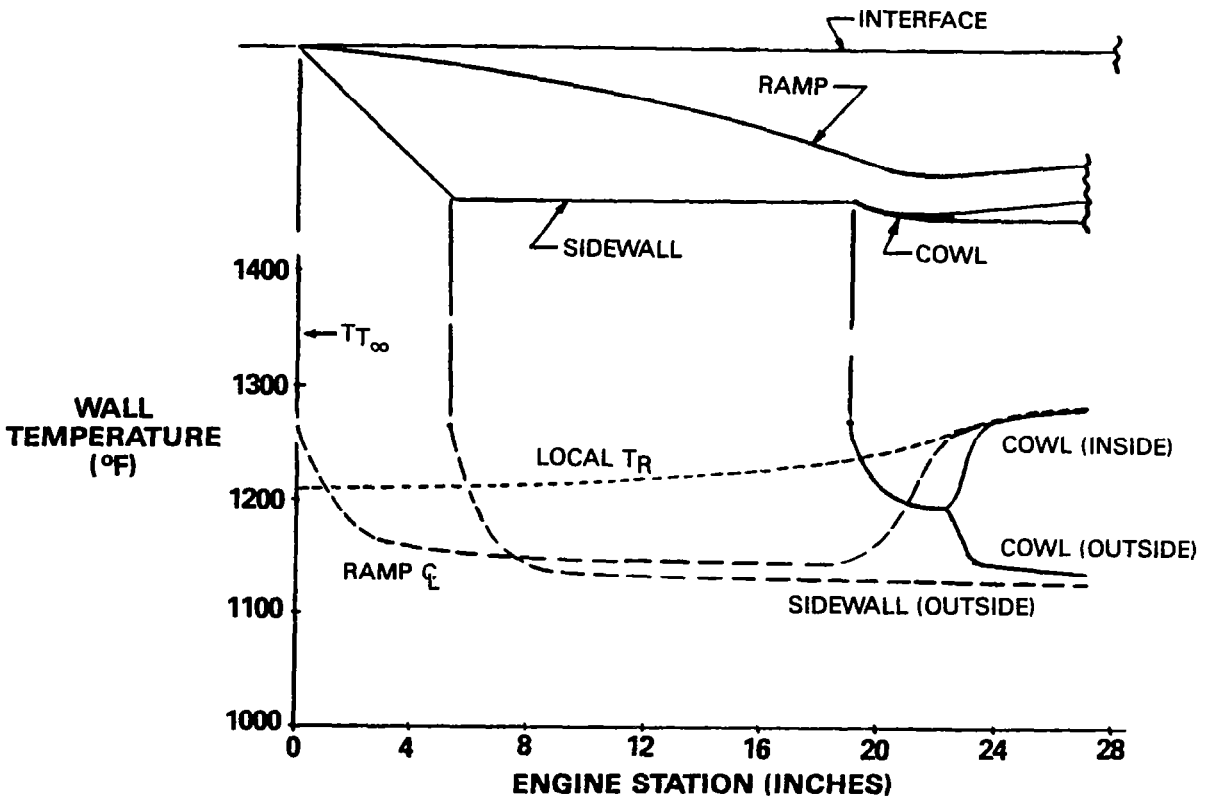

Figure 12. Mach 4, 20,000 Foot Inlet Temperatures, Structural Design Point

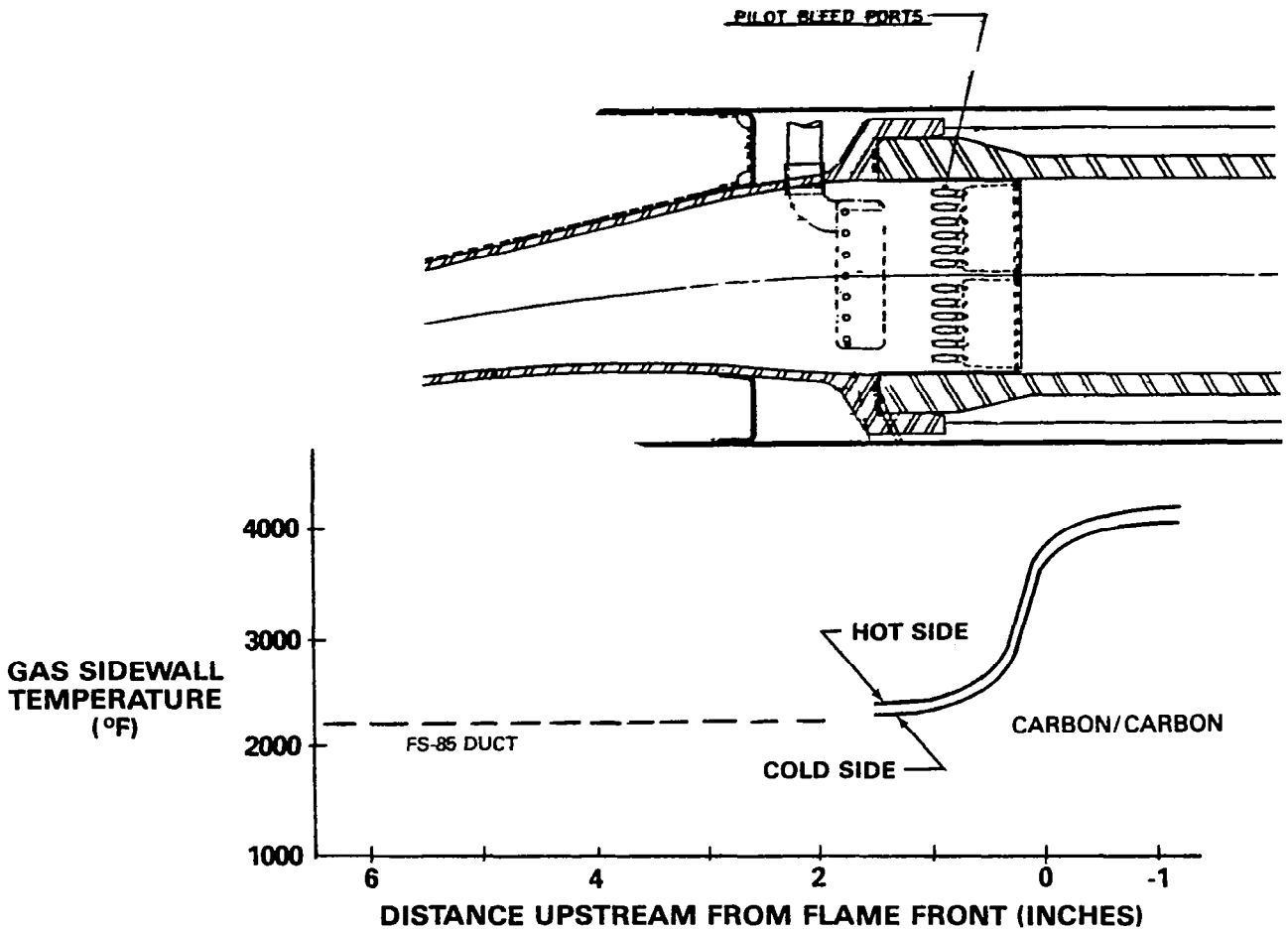

Figure 13. Carbon/Carbon to Columbium Interface

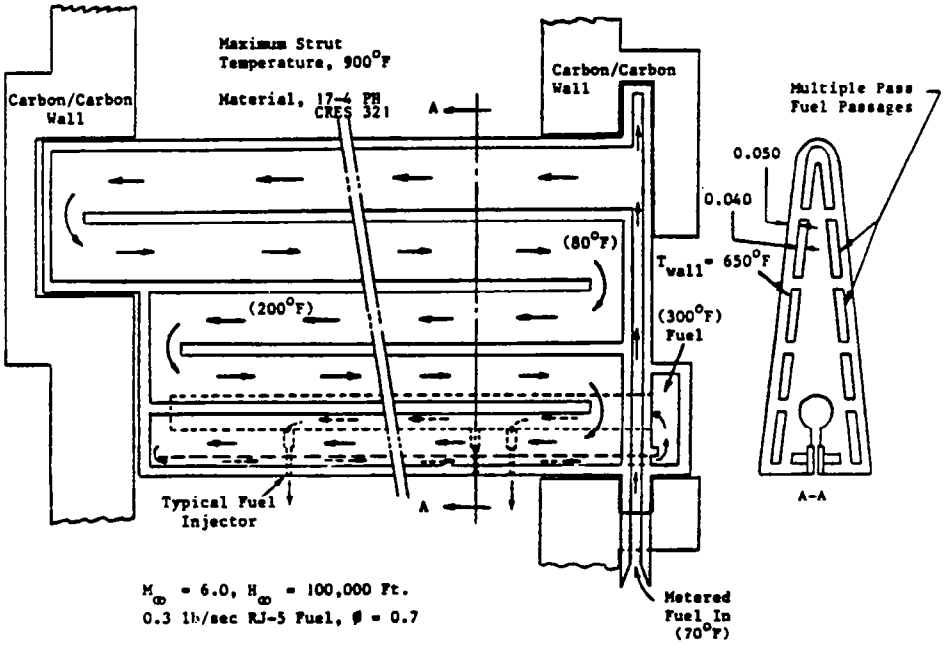

Figure 14. Fuel Cooled Injector Strut

Fuel Cooled Combustor Analysis

A regeneratively cooled combustion chamber, using engine fuel as a coolant, was analyzed to determine if a cold primary engine structure could be provided to ease sealing at joints with hotter component. The concept which was analyzed consisted of a CRES 321 heat exchanger (HX) as the cold outer structure which was thermally protected from combustion gas temperature by a 0.40 inch thick liner. This liner was assumed to be a three-dimensional carbon weave reinforcement with a modified DC93-104 (Dow Corning elastromer) matrix. No erosion of the liner was assumed in the analysis.

The steel HX concept is shown in Figure 15. The outer shell was 0.100 inch thick and the inner shell was 0.06 inch thick. They were separated by 0.270 x 0.075 inch cooling passages, running axially, and formed by 0.075 x 0.100 webs between each passage. The concept was configured to provide a triple pass cooling passage and this geometry provided a fuel coolant velocity of about 3.0 fps at the cruise condition. The concept included an inlet and a discharge fuel manifold which could be integrated into mounting flanges for adjacent components (inlet, c/c combustor/nozzle assembly). A parabolic combustion gas temperature rise was assumed where the gas temperature was inlet total temperature at the upstream end of the HX and combustor discharge gas total temperature at the downstream end of the HX. The HX was 11.5 inches long.

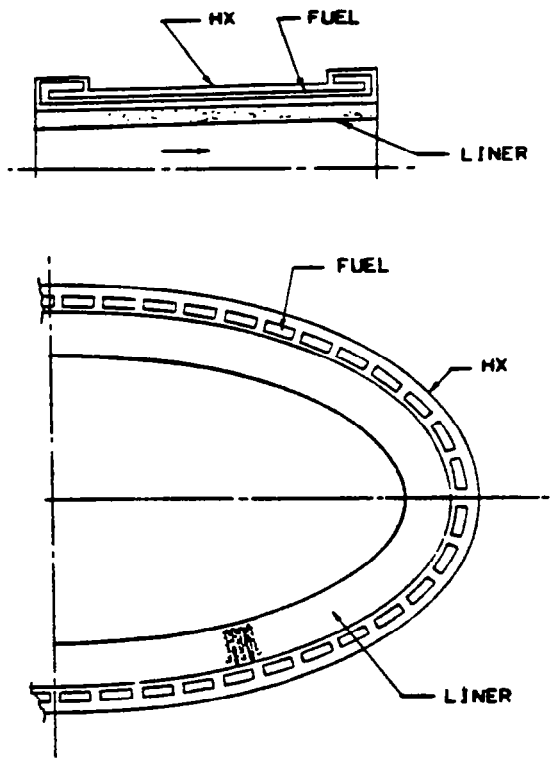

Figure 15. Fuel Cooled Combustor

With 0.30 lb/sec of JP-10 fuel coolant (all of the cruise fuel flow) entering the HX at 70 ° F, the fuel temperature rise through the HX was about 160°F. The hot side HX shell ran about 75°F hotter than the fuel (305°F maximum). The cold side HX shell was essentially at local fuel temperature. Structurally, these temperatures were satisfactory.

There was considerable concern over liner erosion which would increase the heating load on the fuel. When a c/c liner was substituted for the modified DC93-104 liner (retaining 100% surface contact with the HX), the fuel temperature rise was excessive.

Considering the viability of the passive c/c liner, the complexity of the HX and the uncertainty of DC93-104 erosion, the fuel cooled combustor was dropped from consideration in favor of the passive c/c liner. This latter selection, with the carbon felt insulation and the columbium inlet provide an attractive basic design.

STRESS ANALYSIS

The documentation of analyses made to attest the structural integrity of the scramjet engine design (see Figure 6) is presented in this section. Several iterations were required of some of the structural items in order to obtain a strength to weight optimization. Recommendations were made and incorporated into the design in order to optimize the strength-stiffness-weight tradeoffs. A statement of the relevant design criteria, descriptions of various computer analysis models, detail stress calculations, a summary of results and references are included in the discussion.

Discussion

High flight speed and relatively long flight duration combine to create a hostile environment for materials defining the structure of a scramjet. Because missile performance is very sensitive to weight, the need, for optimal structural materials that can reach flight loads within this high temperature environment, is more than apparent. The primary objective here, is to develop and demonstrate the feasibility of a preliminary, but representative, flightweight design operating in a scramjet thermal and flight load environment.

During scramjet operation, the maximum inlet and combustor pressure distributions correspond to low altitude/low Mach number operating conditions. A survey of the overall flight envelope makes it apparent that the pressure loading of the structure drops off at a greater rate than the reduction of temperature dependent material strength properties of the materials selected below. The pressure distribution of Figure 26, is based on a Mach 4 at 20,000 feet flight condition. Since the flight envelope begins with Mach 4 at 25,000 feet, the use of Figure 26, for the maximum operating pressure distribution, is conservative.

Also during scramjet operation, the maximum maneuver loads of 40 "g"s either vertically or horizontally are combined with the maximum operating pressure. The ejection shock vertical load of 61.25 "g's" is an inertial load that occurs by itself.

The basic structural design approach sought here is a hot structure design. Actively cooled and ablatively protected structure designs are to be avoided.

Thermal analysis indicates that the inlet may attain temperatures as high as 2300°F and the outside walls about 1800°F, at the exit. A comparison of the structure temperature capabilities and requirements of materials evaluated, as these temperatures are approached, indicates that the Refractory Metal Alloys and the carbon/carbon are the only structural materials capable of these temperatures. The open shape of the 2D inlet design promotes large bending moments and shear loads at the corners. This alone is enough to eliminate carbon/carbon from consideration for the inlet design. In this realm of temperatures, refractory metal alloys exhibit superior bending strength to weight to available space usage characteristics over carbon/carbon.

Tantalum and columbium are the primary refractory metals used in this temperature regime. Tantalum T-222 provides the best combination of properties of the tantalum alloys. C129Y is a high strength columbium alloy with good resistance to creep. FS-85 columbium has a slightly lower yield strength at room and elevated temperatures than C129Y, however, FS-85 is preferred over C129Y, because of its relatively good formability and weldability characteristics at room temperature. Between room temperature and 1600°F, FS-85 is superior to T-222 for a strength/weight comparison, while above 1600°F the roles are reserved. The design temperature of the inlet is 1200°F. Therefore, FS-85 is selected as the principal choice for the material to be used for the inlet and airframe structures. Columbium C-103 appears to be a logical choice for the inlet and airframe, but at T = 1200°F, when reacting bending, structural components made of C-103 are 19.5% heavier than those made of FS-85. When reacting tensile loads, structural parts made of C-103 are to 70.9% heavier than those made of FS-85. But, C-103 will provide lighter shear panels than FS-85 columbium, for a semi-monocoque design concept. In order to prevent oxidation, VH109 silicide coating is suggested as a surface protection of the FS-85 columbium. VH109 exhibits good characteristics up to 3000°F.

The combustor-nozzle assembly presents another problem. The thermal analysis indicates that the combustor may reach temperatures as high as 4300°F. Carbon/Carbon composite is the only material capable of withstanding these temperatures.

The use of carbon/carbon materials in the integral throat and entrance portion of solid rocket motor nozzles has become a state-of-the-art technology.

Some use of carbon/carbon is seen on exit cones. McDonnell Douglas, St. Louis, Missouri, has built and tested combustors with walls of 2D braided carbon/carbon and 3D matrix full depth woven carbon/carbon.

The geometry of each one of these has one thing in common: axisymmetry. No circumferential bending is present. When pressurized, the scramjet elyptical 2D combustor cross-sectional geometry lends itself to generating relatively high circumferential corner stresses. For the preliminary effort dealing with sizing the chamber-nozzle, 2D braided and 3D carbon/carbon material properties supplied by McDonnell - St. Louis, Mo. were used. The following stress analysis, based on these properties, indicated that 2D braided carbon/carbon would require too great of a thickness in order to withstand the flight loads. Therefore, a 3D full depth weave carbon/carbon, chamber wall with an internal and external pyrolytic graphite coating to prevent oxidation and erosion is selected for the combustor-nozzle. The 3D carbon-carbon fiber reinforced composite material has been idealized as a homogeneous material which has orthotropic material properties; such that the Hooke's law relationship in a plane stress state is

$$\begin{Bmatrix} \sigma xx \\ \sigma yy \\ \tau xy \end{Bmatrix} = \begin{bmatrix} Cxx & Cxy & O \\ Cyx & Cyy & O \\ O & O & Gxy \end{bmatrix} \begin{Bmatrix} Exx \\ Eyy \\ xy \end{Bmatrix}$$

A weight-strength tradeoff has been made based on the existing design, which indicates that a promising design geometry has been reached. The analysis, which results in the tradeoff, has been built on worst case combinations of maximum operating pressure, differential thermal expansion, and maneuver loading of the chamber. The burst pressure by itself has also been an important design condition. Several computer runs were made which involved chamber wall thickness iterations over specified lengths of the chamber. The recommended optimization of the chamber is shown in Figure 16 including the assumed 3-D carbon-carbon material properties.

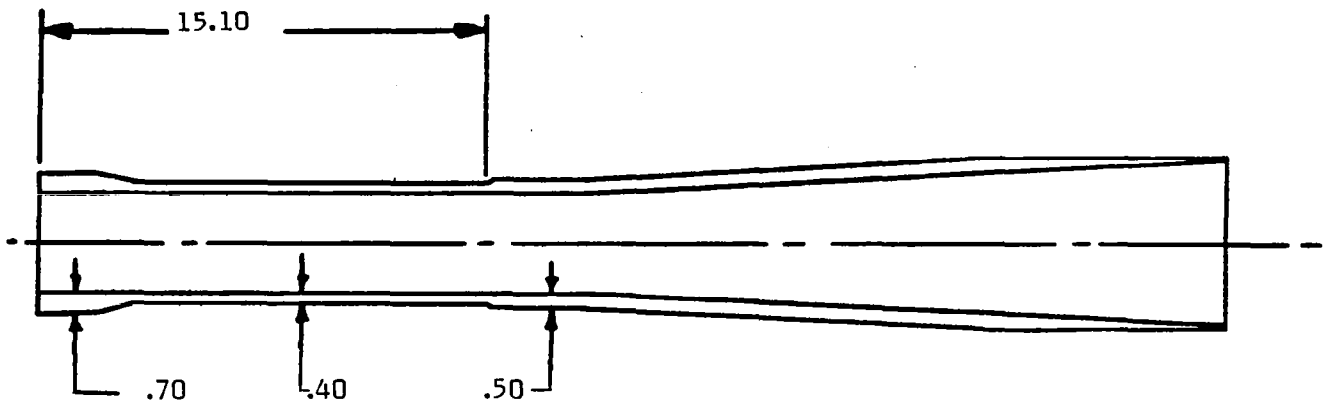

	Circumferential (YY)	Longitudinal (XX)
Tension	46,000 psi	21,000 psi
Compression	15,600 psi	14,600 psi
Flexural (Flat)	28,700 psi	21,000 psi
In Plane Shear	2,150 psi	2,150 psi
Flexural Shear	4,060 psi	3,930 psi
Young's Modulus	15.9E6 psi	4.5E6 psi
Shear Modulus	.6E6 psi	.6E6 psi
Poisson's Ratio	.2	.2

Figure 16. Chamber Wall Thickness and Material Properties

The model used for the stress analysis of the 2D inlet is a finite element model. The computer program used for this work is SAP V. Type 6 thin plate elements were predominately used to represent the inlet. The structure is represented by a half model for computer time economy. The 2D inlet is symmetrical about its centerline. Therefore, with the appropriate use of boundary elements, it is convenient to model only half of the structure as shown in Figure 17.

High density plate elements are used in areas of predicted peak stresses with the remainder of the model kept simple to permit economical computer time usage. In order to load the internal plate elements with a representative pressure loading, an axially dependent differential pressure grid was developed. This grid was placed over the layout of the model, and the differential pressure at the center of each element was read and entered in the input format. For this analysis, all of the FS-85 plates of the inlet are considered to be welded together.

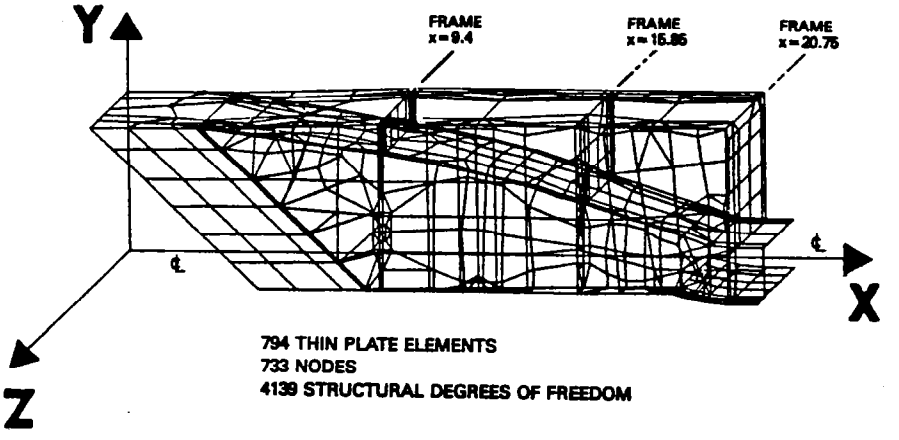

Figure 17. Scramjet 2-D Inlet Finite Elements Model

The role played by the monocoque shell structure is a multi-faceted one. First it must act as an outer fairing to the Mach 4 to 6 air stream. Secondly, it must act as a beam which reacts inertial loads from the overall engine mass distribution. And thirdly, it must be designed so that the severe temperature environment of the chamber will not hurt the shell and the vehicle that the engine is providing propulsion for.

An analysis was conducted to substantiate the structural integrity of the monocoque shell. In order to do this, the shear and moment diagrams for a one g inertial load must be developed. In order to develope the diagrams, the reactions to the mass distribution must be first calculated. Since the engine is hung from the vehicle at the forward and aft supports, shown in Figure 18, the force reactions due to vertical and horizontal loads are easily obtainable.

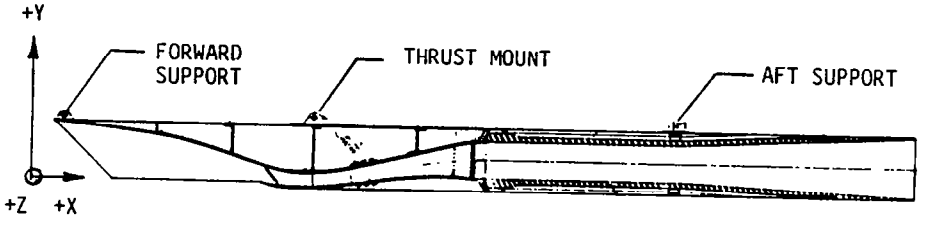

Figure 18. Engine Mount Location

But, since the horizontal loading also entails torsional reactions at the forward and aft supports, determination of the redundant torsional reactions becomes somewhat cumbersome. The torsional sections of the engine varys between single cell torque boxes to three cell torque boxes.

The assembly of ribs, frames, aft portion of the inlet, and the monocoque shell, shown in Figure 19, serve as a system of redundant load paths transferring the carbon-carbon chamber thrust loads into the thrust mount and then into the vehicle itself. A crude, but representative finite element model of this assembly has been run which uses the thrust load obtained from the meridional membrane output stresses from the pressurized chamber work. The stress distributions have been obtained and detail stress analysis of the critical load paths performed.

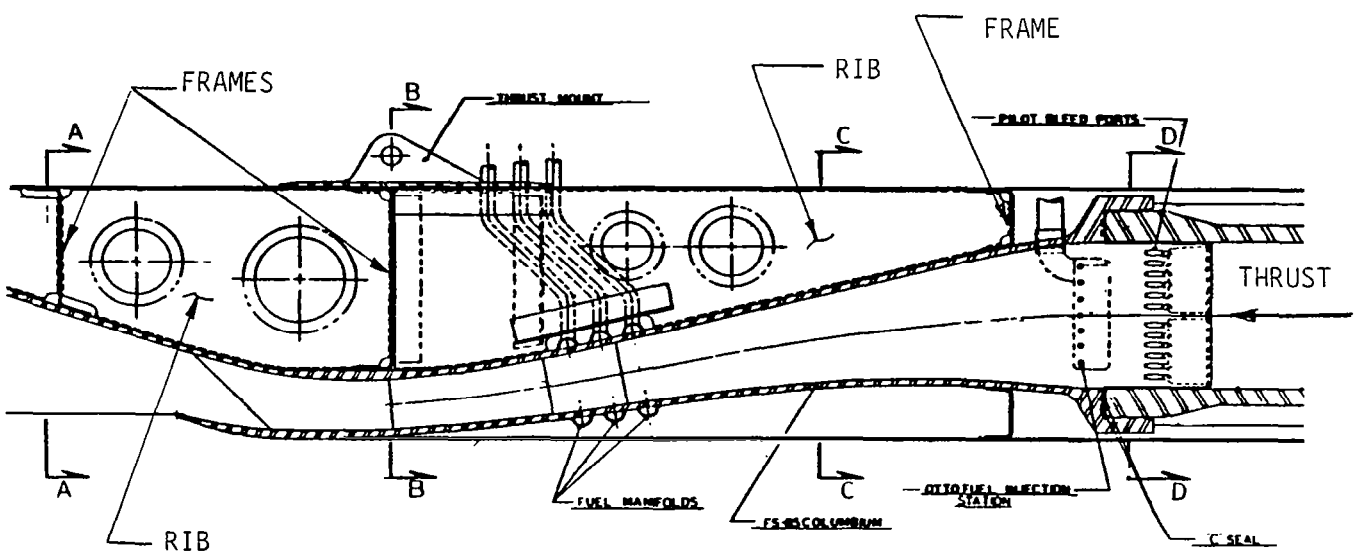

Figure 19. Engine Inlet Structure

The forward end of the carbon-carbon chamber is subjected to a severe thermal gradient in the meriodional direction. This gradient initiates in the region of the flame front, such that differential thermal expansion of the chamber leads to significant stresses in this local area.

A design concept joining the diffuser/combustor assemblies is shown on Figure 19. The columbium retainer, which reacts thrust from the carbon-carbon chamber, captures the chamber. Because the columbium has a higher coefficient of thermal expansion than the carbon-carbon, the columbium will expand away from the carbon-carbon, and thusly avoid differential thermal expansion loads at their interface.

Much concern has been expressed over relative deflections, between the carbon-carbon chamber and the monocoque shell, due to operating environment conditions. The operating environment includes deflections due to maneuver loading and maximum operating pressure loading. The deflections were determined at the aft support, which is about half way between the ends of the chamber supports. The original design shows an insulator block here which is intended to give some support to the chamber, Figure 20. The analysis has been performed as if the insulator block is not there.

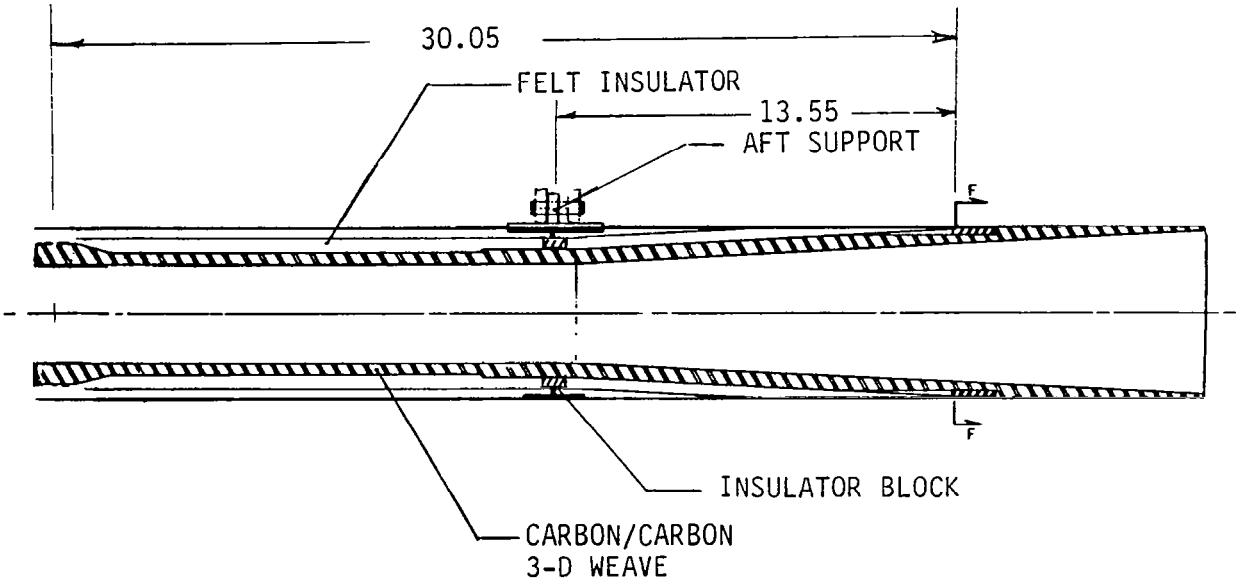

Figure 20. Combustion Chamber Support

The monocoque shell can be idealized as a simple supported beam which is supported at the fwd and aft supports. The shell and the chamber will have the same deflections at the two stations where the chamber is supported.

Summary of Structural Analysis

A summary of the margin of safety of the major component parts is presented in Table 1. Following Table 1 are brief reviews of the analysis of each component.

TABLE 1. SUMMARY OF MARGINS OF SAFETY

(NOTE: THESE MARGINS ARE BASED ON RECOMMENDED CHANGES)

ITEM/SUB-ASSY	MINIMUM MARGINS OF SAFETY	MATERIAL	DESIGN CONDITION	CRITERIA FOR MARGIN OF SAFETY
Combustion Chamber	+.23	3D Carbon/ Carbon	Maximum operating pressure combined with 40 g maneuver	TSAI-Hill failure criteria
	+.23		Burst pressure condition	TSAI-Hill failure criteria
Monocoque	+.31	Columbium C-103	Ejection shock at T = 1200°F	Local buckling of the monocoque shell @ x = 38.75, and @ x = 57.25
	+.24			
Chamber to Shell Deflections	+ Large	-	Maximum operating Pressure combined with 40 g maneuver	Small deflections indicate the chamber and shell are fairly rigid with respect to each other, and no mid-supports are required.
Thrust Reaction Structure/ Ribs Between x=33.46 & 38.75	+.49	C-103	Reacting Maximum operating pressure thrust from the carbon/carbon chamber @ T=1200°F	Combined shear and compressive buckling
Between x=23.85 & 33.46	+.07			
2D Inlet/ Ramp Top	+.16	FS-85	Maximum operating pressure @ T=1200 F	Plate bending @ Fty
Frame @ x=9.40	+.04	FS-85	Maximum operating pressure @ T=1200 F	Frame bending @ Fty @ Frame Corner
Frame @ x=15.85	+0.0	FS-85	Maximum operating pressure @ T=1200 F	Frame bending @ Fty @ Frame Corner
Roof Top	+.94	FS-85	Maximum operating pressure @ T=1200 F	Plate Bending @ Fty
Ramp Side	+.10	FS-85	Maximum operating pressure @ T=1200 F	Plate Bending @ Fty
Outside	+1.67	FS-85	Maximum operating pressure @ T=1200 F	Plate Bending @ Fty

Summary of Combustor Analysis

In order to optimize weight vs. strength of the 3D carbon-carbon chamber the wall thicknesses were determined. The critical margins of safety for a burst pressure loading of this configuration are found below in Figure 21.

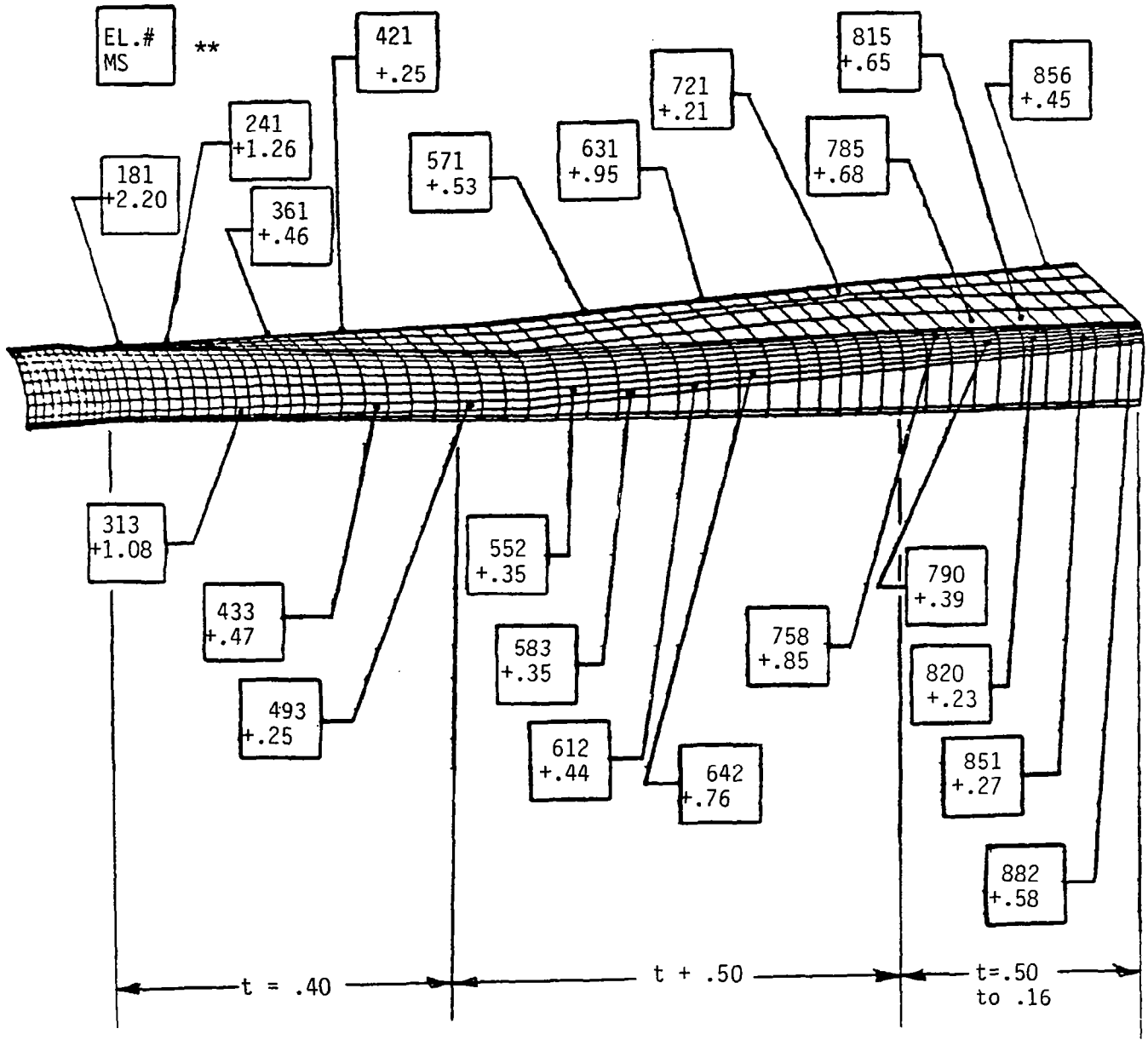

Figure 21. Summary of Margins vs Element Locations for Burst Pressure Condition

During free flight operational loading conditions, it is seen that the region of the chamber, which experiences high stresses due to differential thermal expansion, receives comparatively low stresses from both inertial and pressure loading. The most severely stressed element is 164 shown in Figure 22, where

MS = +.47

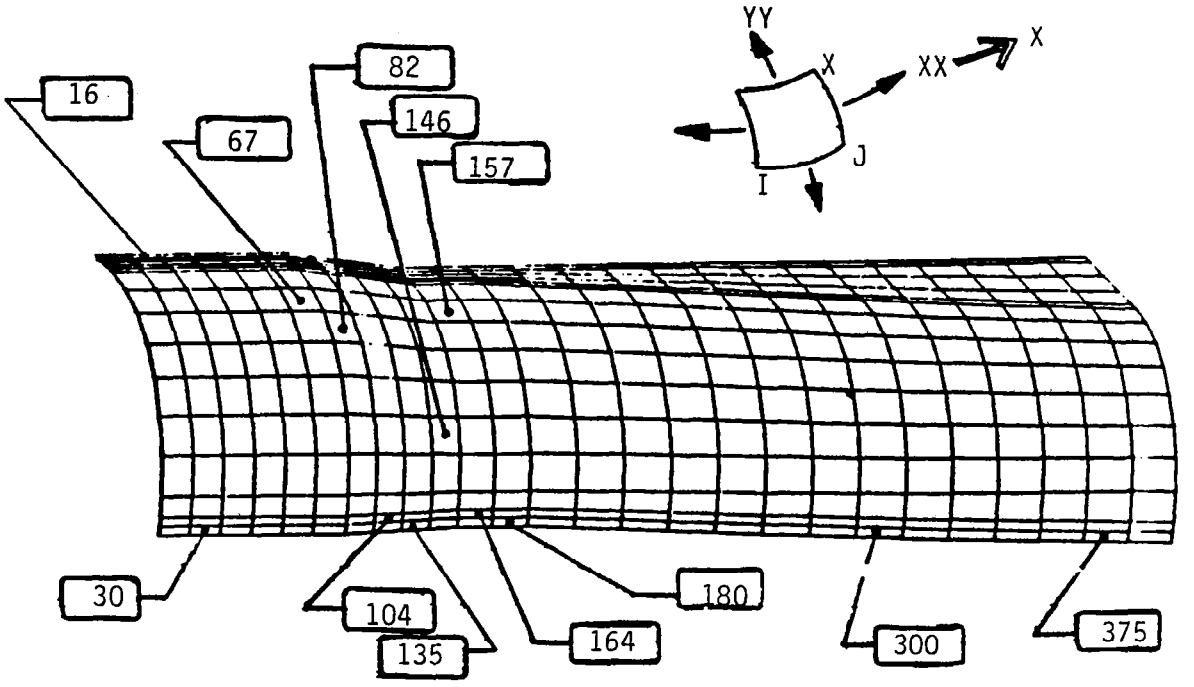

Figure 22. Location of Critical Stresses

Further down the chamber, where the differential thermal expansion stresses are negligible, the combining of pressure and inertial loads, results in

MS = +.23 at El. 421

Summary of Monocoque Shell

Referring to the propulsion unit moment diagram of the analysis, the maximum bending moments reacted by the monocoque shell are at X = 38.75 & X = 57.25. The ejection shock condition is the critical design load case, where

m' (38.75) = 89,813 in lb

m' (57.25) = -21, 254 in lb.

The monocoque shell is local buckling critical at these sections.

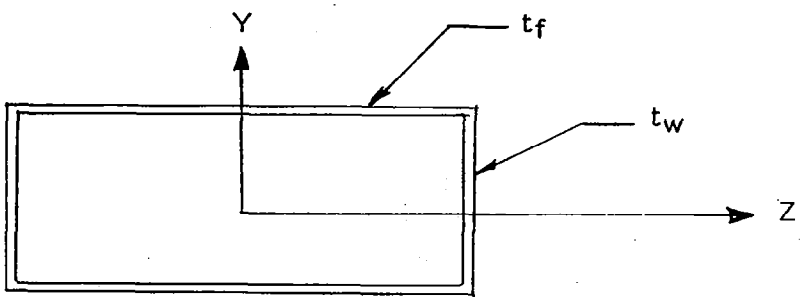

If the shell must be monocoque, the recommended columbium C-103 material thicknesses are:

t_f = .125 in.
t_w = .090 in. at x = 38.75 MS = + .31

tt_f = .100 in
tt_w = .070 in. at x = 57.25 MS = + .24

It is recommended that the outer shell structure be a semimonocoque shell. It is not feasible to have the shell thick enough to resist compression loads. In semimonocoque structures, the thin webs resist tension and shearing forces in the planes of the webs. The stiffeners (or cap areas) resist the compression forces in the plane of the web. Therefore, the addition of correctly sized corner angles to the shell would reduce the wall thickness and the weight of the shell.

Summary of Chamber to Shell Deflections

The maximum change in the gap between the chamber and the monocoque shell directly beneath the aft support of the shell is

Δgap = .0128 + .002 + .0259

Δgap = .0407 in. due to a 40g maneuver occurring simultaneously with maximum operating pressure.

Only 35% (.0148) of Δ gap is due to inertial loading. This tells us that the chamber and shell are fairly rigid with respect to each other, and the insulator block is not required. (see, Figure 20).

Summary of Thrust Reaction Structure

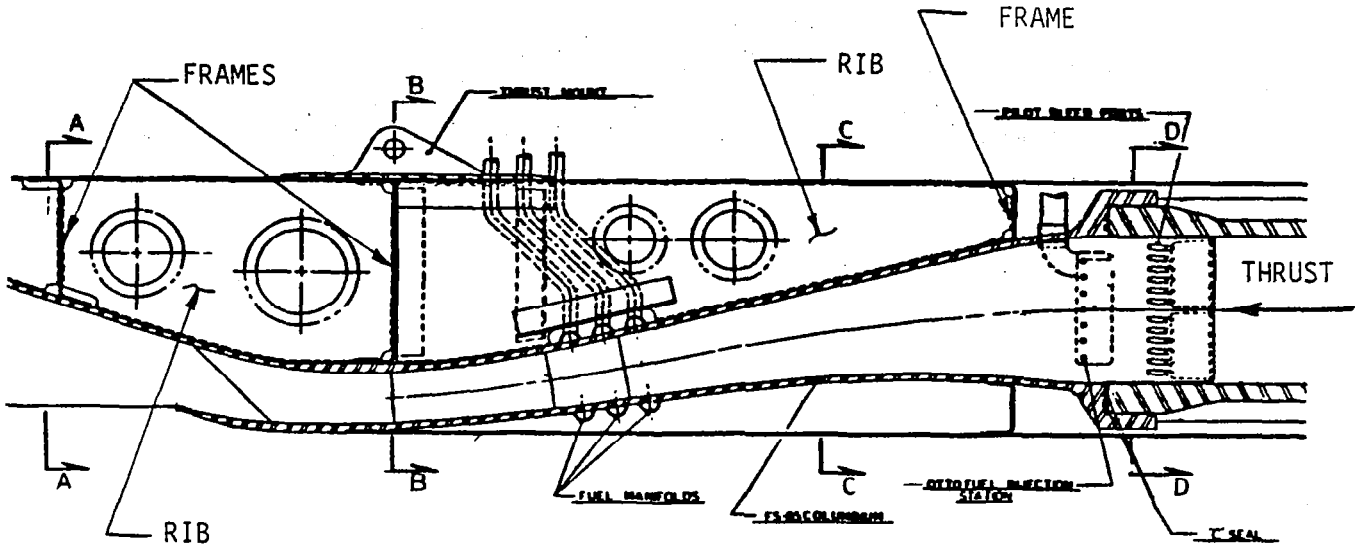

Figure 23. Thrust Reaction Structure

The recommended material thicknesses for the C-103 ribs are:

Between x = 23.85 & 33.46 ⟶ t = .050 and the design modifications

MS = + .07

Between x = 33.46 & 38.75 ⟶ t = .040 and the design modifications

MS = + .49

Summary of Results of 2-D Inlet

Except for the following recommendations, the 2D inlet design is optimal for strength to weight tradeoffs. The design criteria is based on tensile yield at a maximum operating pressure condition.

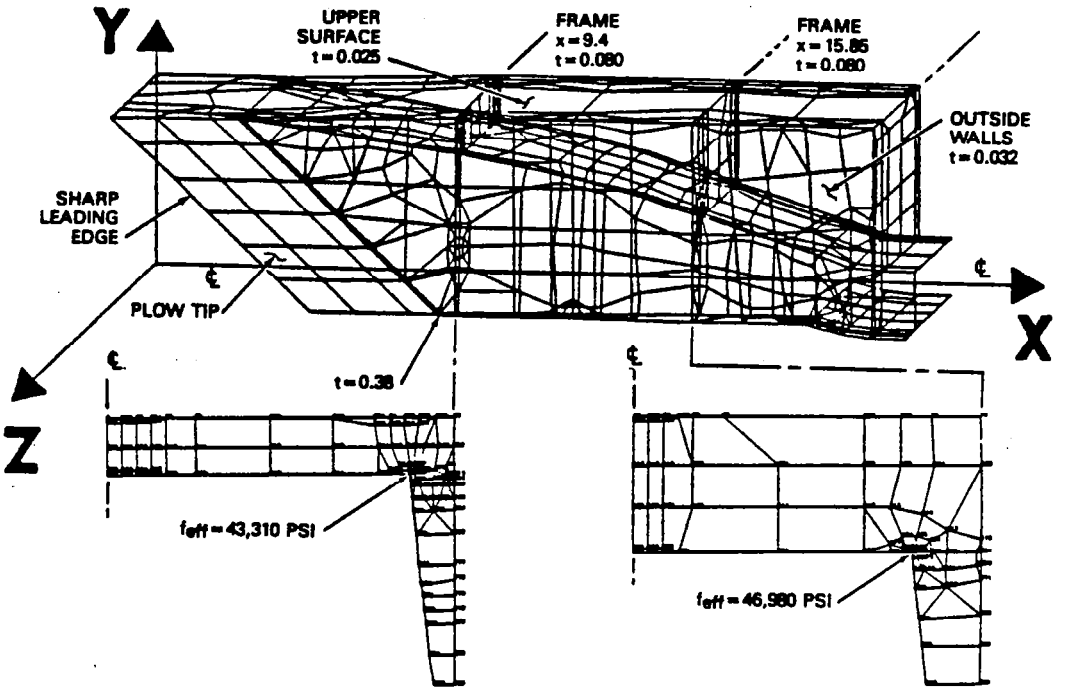

Figure 24. Inlet Model Skin Gauge Definition

It is recommended that the ramp top have a thickness of .125. We have no analysis indicating how thin the ramp top may be with the addition of ribs.

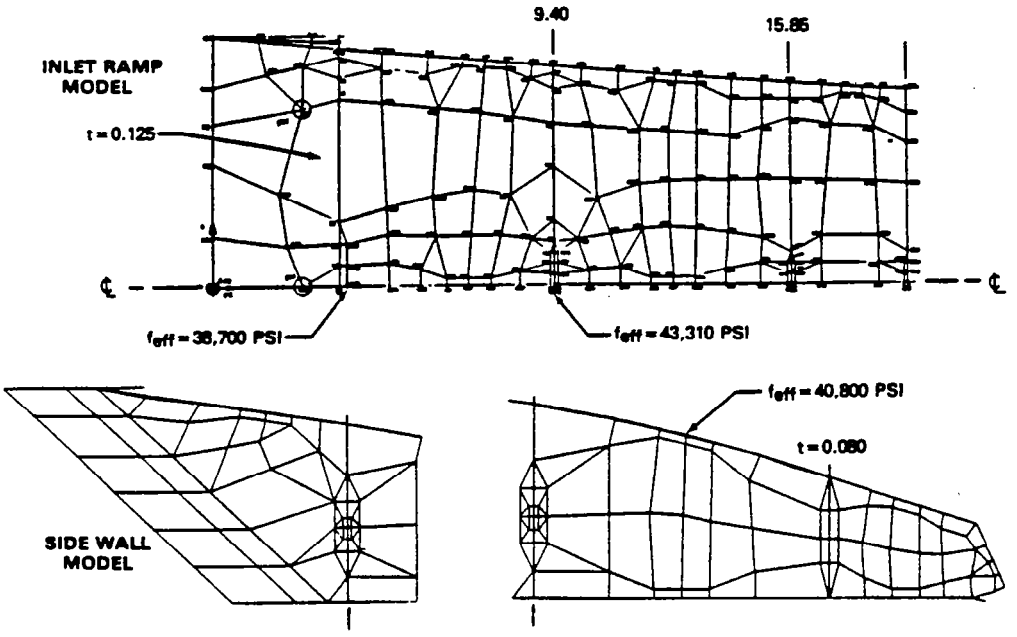

Figure 25. Inlet Ramp and Sidewall Model

STRUCTURAL CRITERIA

Since this feasibility study is not constrained by a set of operational loads and factors of safety, we have arbitrarily selected some stringent requirements which were used in previous ramjet programs here at Marquardt. This section spells out the rules that bind the structural analysis of the scramjet propulsion system.

General Geometry

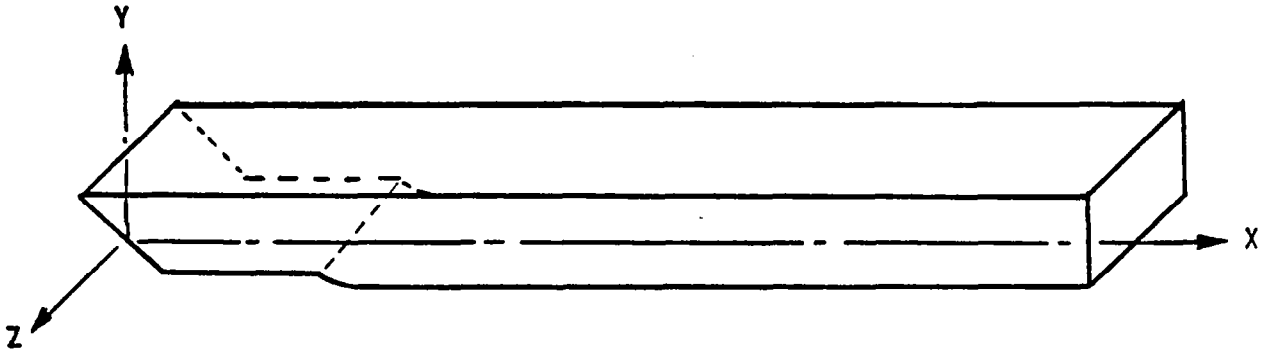

Design Criteria

Scramjet Operation:
Proof = 1.00 x maximum operating
Burst = 1.25 x maximum operating

Load - Pressure Combinations:
Proof and burst pressures not combined with mechanical loads.
Maximum operating pressure combined with mechanical loads.

Factors of Safety:
F.S. = 1.25 (ult.) for free-flight conditions
F.S. = 1.50 (ult.) for captive carry, airlaunch ejection.

Shock - Ejection Shock (35G, 30 ms, half sine pulse)
Max G (response) = (1.75) (35g)
= 61.25g
Applied perpendicular to the longitudinal axis in the Y-direction.

Free Flight Maneuver - 40G maneuvers both vertically and horizontally over the operating envelope.

Maximum operating pressure is shown in Figure 26.

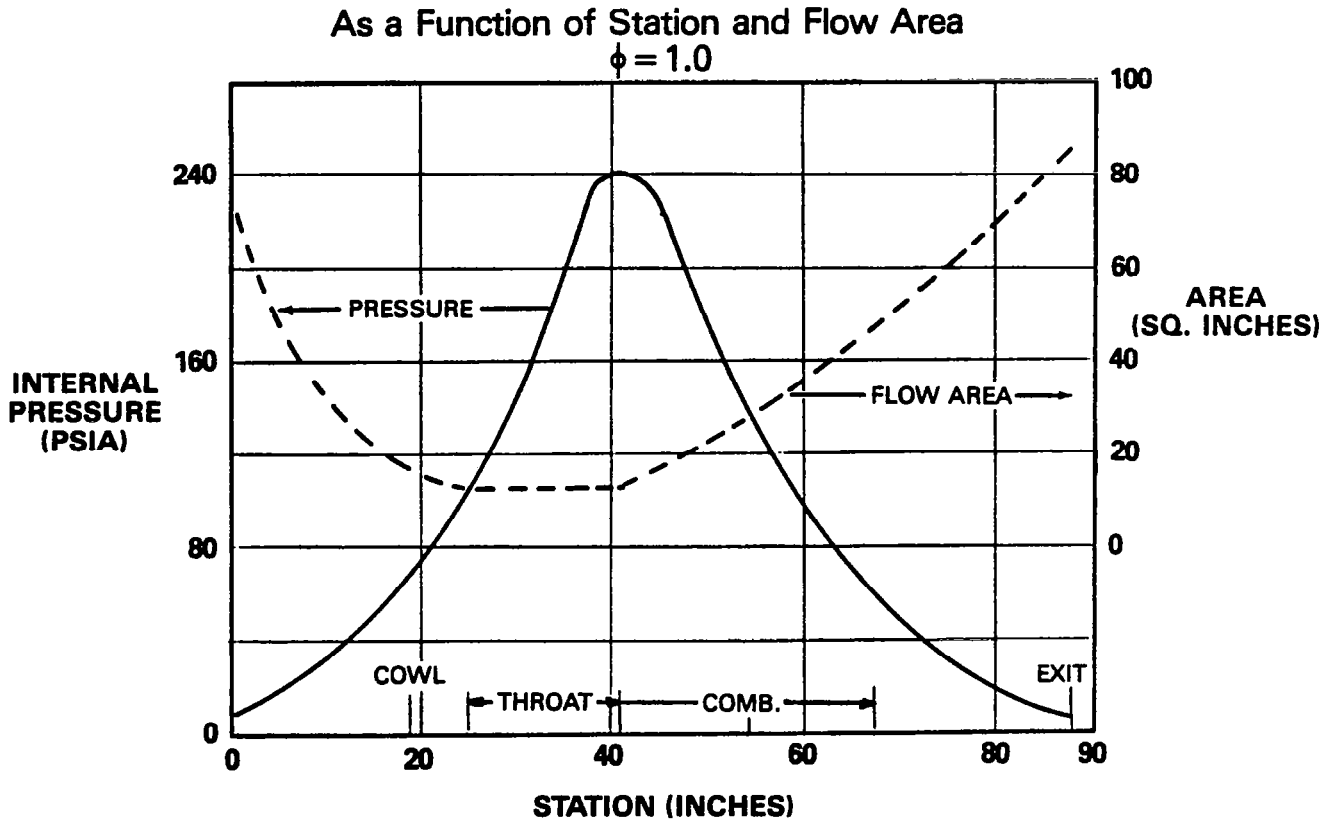

Figure 26. Mach 4, 20,000 Foot Internal

Pressure Distribution

CONCLUDING REMARKS

The preliminary design of a scramjet engine based upon the environment prescribed by the HYSAM flight trajectory has been addressed. A feasible concept was defined which uses state-of-the-art materials and the technology established by The Marquardt Company during previous development programs. Component changes should not alter the validity of this analysis.

A detailed structural analysis was conducted along with an indepth thermal analysis. Structurally all the components within the system exhibit positive margins of safety. The thermal analysis of the engine indicates that a thermally viable configuration exists.

The engine basically consists of a three-dimensional carbon/carbon (c/c) combustor/nozzle liner secured to an FS-85 columbium inlet. The c/c liner is sheathed with carbon felt insulation to thermally protect the FS-85 engine structure and skin. Fuel is injected into the engine air flow about midway between the inlet cowl and the forward end of the c/c liner. The OTTO II ignition/sustaining agent is injected from a strut near the loading edge of the c/c liner.

A development program should now be pursued addressing indepth the design, the structural, the thermal analysis and the performance of this airbreathing propulsion system capable of operating in the hypersonic speed regime.

APPENDIX A

INLET CONCEPTS STUDY

Inlet Concept Trade Study

Three scramjet inlets for application to the Wide Area Defense Missile configuration have been examined. The vehicle has a flat bottom on which the inlet and scramjet engine are mounted. The inlet configurations studied were dictated to a large extent by the requirements that the vehicle, including the inlet, fit into the 22 by 22-inch vertical system launch. (Figure 1). The three inlets studied were

1. Half axisymmetric with bypass.
2. Half axisymmetric without bypass.
3. Three-dimensional scoop.

A two-dimensional inlet (rectangular cowl shape) was previously examined. This inlet does not produce sufficient capture area because of the launch tube constraints. A comparison is shown in Figure 2 of the predicted capture area ratios of each configuration.

The general philosophy and guidelines for the design of a fixed geometry scramjet inlet is discussed in this paragraph. It is assumed that the inlet has to operate over a range of Mach numbers and be capable of accelerating from some low Mach number to some high Mach number. In this case, a high capture area ratio over the Mach range is desirable. Total pressure recovery is not as important for a scramjet as for a subsonic combustion ramjet, but reasonably high pressure recovery is desirable. Low inlet drag is also desirable. For a fixed geometry inlet the overall contraction ratio should be as high as possible, compatible with starting the inlet at the minimum operation Mach number high contraction gives low Mach numbers at the combustor entrance, thus minimizing total pressure losses due to heat addition. High contraction, however, also produces high static pressure in the inlet and combustor which may be undesirable structurally. The inlet lines determination should be amenable with inviscid flow theory. Although the inlet lines are determined at one Mach number, the resulting shape is usually suitable over a range of Mach numbers. Also, the inviscid flow properties serve as input to viscous flow computation. Viscous phenomena is very important in scramejet inlets. At very high speeds (M = 6 and higher), skin friction will be the major contributor to total pressure losses. Boundary layer separation, for example, can result in loss in pressure recovery, lower capture area ratio, local hot spots back burning and in some cases inlet unstart. Boundary layer separation is caused by high flow compression rates (i.e., high negative dp/dx); for example an impinging or generated shock wave. Rapid expansion, such as a sharp corner, can also produce boundary layer separation. Therefore, both rapid expansion and compression should be avoided; this however, results in longer inlets. Boundary layer separation can be prevented in some cases by proper use of bleed and/or tripping devices (to create turbulent flow). Blunt leading edges are usually necessary due to high heating rates associated with sharp leading edges. Blunt leading edges create shock waves which may result in boundary layer separation and the problems discussed above. Highly swept leading edges require less bluntness and should be used where possible. Internal compression alone is usually insufficient to produce the desired contraction ratio because of inlet starting requirements. External compression alone results in high cowl drag and/or strong internal shock waves. Mixed (external and internal) compression is generally best. A bypass/bleed system will permit relatively high external compression with low cowl drag as discussed below.

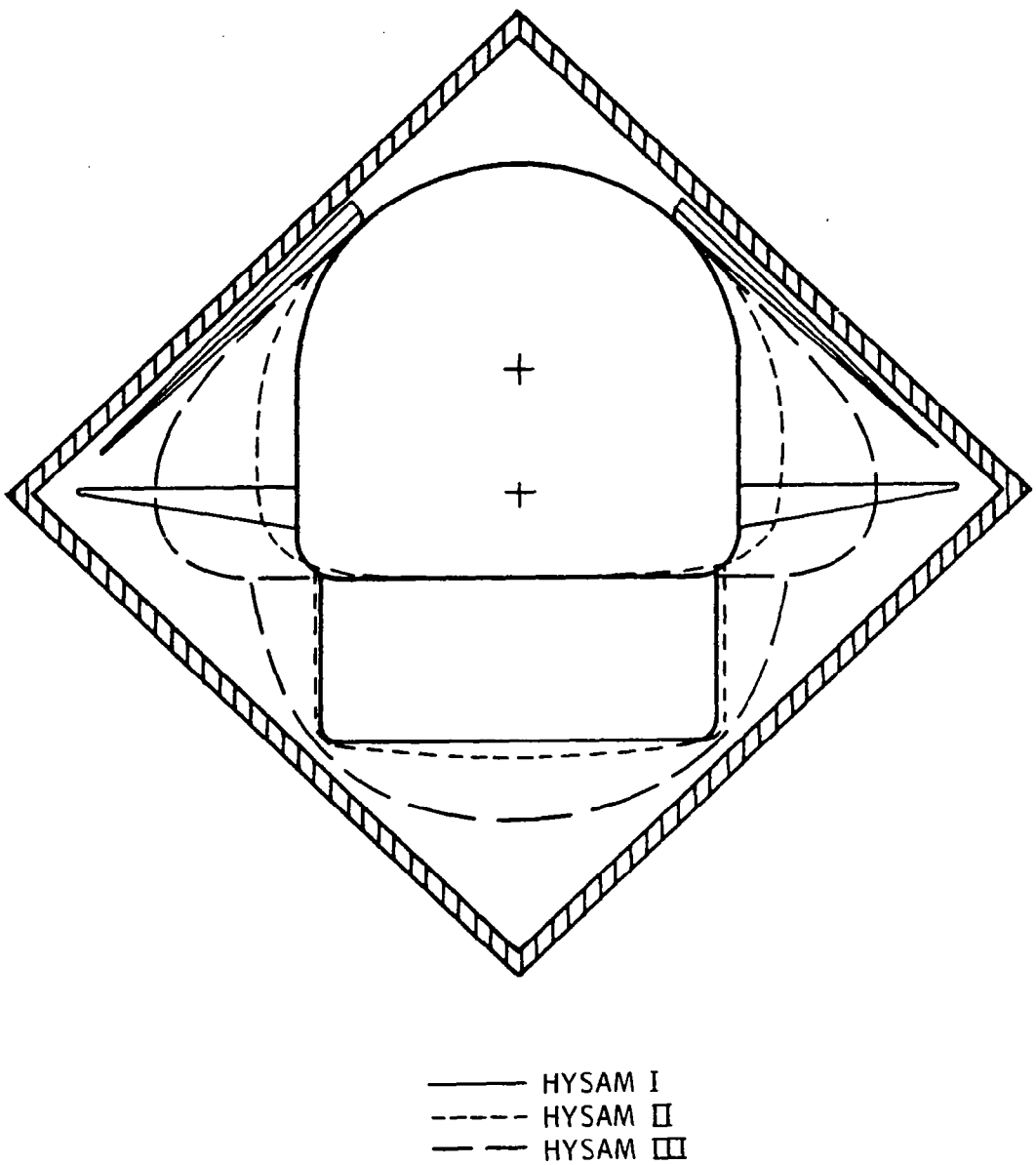

Figure 1. Vertical Box Launcher Cross Section

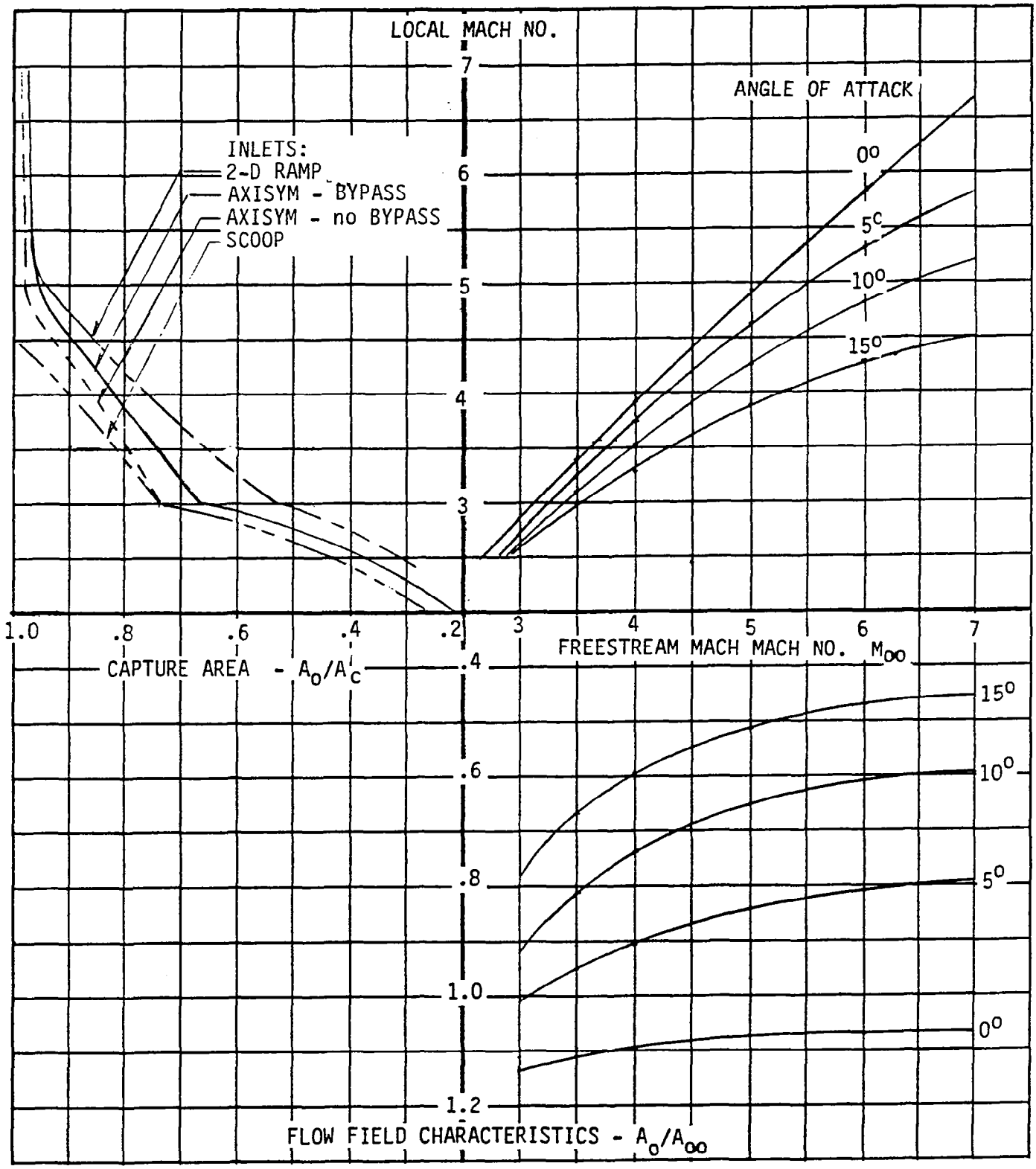

Figure 2. Comparison of Various Inlet Capture Area Ratios Ao/Ac

Half Axisymmetric Inlet with Bypass

This inlet was selected for investigation because (1) compatibility with the vehicle and launch tube and (2) the inviscid flow can be analyzed using the axisymmetric method of characteristics. The compression is mixed but primarily external.

The initial compression surface is a 10° half cone followed by a half axisymmetric isentropic compression surface. The initial conical shock wave is on the cowl lip at Mo = 5 and the isentropic compression waves focus on the cowl lip at Mo = 3.5. This technique gives higher capture area ratios at lower Mach numbers compared to a conventional inlet (where both the shock and compression waves focus on the cowl lip at the design Mach number) designed for a high Mach number. The amount of compression and total pressure ratio are the same as a conventional design. The only penalty for this technique is that the isentropic compression on the spike is more rapid and will probably require bleed to prevent boundary layer separation or bridging.

The initial cowl angle is relatively flat (16.1° for an external flow angle of 32.1° at Mo - 3.5). This reduces cowl drag considerable compared to a flow aligned cowl. The resulting internal shock wave has an initial deflection angle of 16° which would normally cause boundary layer separation. This shock is cancelled by a corner on the innerbody at the downstream end of the bypass duct. Separation will not occur due to the shock impingement since the bypass duct has removed the boundary layer.

The primary purpose of the bypass is to remove boundary layer which permits a strong internal cowl shock and lower cowl drag. The bypass also helps starting at low Mach numbers. Boundary layer removal will prevent separation and maintain more uniform flow in the inlet duct downstream of the bypass. The bypass is thought to be necessary particularly since the inlet ingests the vehicle forebody boundary layer. The bypass/inlet lines are such that inviscidly no flow would enter the bypass. Thus the flow through the bypass is primarily boundary layer and the flow rate is low. This approach to the bypass design requires a Prandtl-Meyer expansion at the upstream end of bypass duct. This causes the inlet to turn inward. Approximate inlet lines are shown in Figure 3. The section following the inlet is a transition duct that changes the shape from an annular cross section to a circular cross section at the combustor entrance. The ground rules for designing this section are that it be constant area and that the changes in slope be gradual.

Performance estimates and inlet constants for the half axisymmetric bypass inlet are given in Table I.

The bypass momentum recoveries shown in Table I have been reduced by 50 percent of the estimated value for a well designed bypass duct to allow for driving an air turbine. This causes the bypass drag to approximately double. Bleed will probably be needed on the external compression surface which can be determined experimentally. The cone tip, cowl lip and leading edge on the bypass duct should be roughened to encourage the boundary layer transition from laminar to turbulent flow.

TABLE I - CONT.

COORDINATES - HIGH COMPRESSION HALF
AXISYMMETRIC INLET WITH BYPASS DUCT

Spike

x	y	
0	0	10°
19.53	3.444	
21.582	3.842	
23.634	4.311	
25.686	5.063	
27.738	6.308	St Line
29.105	7.301	

Cowl Internal

x	y	
28.637	8.000	Parabola — Tangent to 16.127°
29.636	8.233	Parabola — Tangent to 10.127°
31.419	7.695	St Line -38° — Tangent to -38°
32.564	6.800	

Centerbody

x	y	
29.105	7.301	Bypass Gap — Tangent to 36°
29.984	7.234	Parabola — Tangent to -16°
32.044	6.134	Tangent to -38°

Bypass Upstream

x	y	
29.105	7.301	St Line -35°
29.726	6.866	

Bypass Downstream

x	y	
29.984	7.234	- Tangent to -35°

TABLE I - Half Axisymmetric Bypass Inlet

External Compression - 10° half cone (blunted)
36° total turning on spike
32.1° flow angle at cowl lip

Contraction - Overall, Ac/A_2 = 5.86
External, Ac/A_1 = 5.00
Internal, A_1/A_2 = 1.17

Areas - Ac = 100.53 sq. in. (Rc = 8 inches for half inlet)
A_1 = 20.11 sq. in.
A_2 = 17.17 sq. in (Equivalent diameter = 4.676 inches)

Shock on cowl lip at Mo = 5, compression waves on cowl lip at Mo = 3.5

Cowl Lip - Blunted, d = 0.125. External and internal angle = 16.1°

Cowl internal shock strength = 16°

Mo	$\frac{Ao}{Ac}_T$	$\frac{Ao}{Ac}_B$	$\frac{Ao}{Ac}_P$	M_2	$\frac{P_{T2}}{P_{To}}$	KE_2	MR_B	C_{DB} *	C_{DA} *	C_{DC} *	C_{DT} *
3.0	0.740	0.067	0.673	1	0.896	0.982	0.450	.0732	.0151	.0903	.1786
3.5	0.795	0.049	0.746	1.65	0.832	0.978	0.421	.0564	.0113	.0424	.1101
4.0	0.857	0.039	0.818	2.06	0.794	0.979	0.407	.0461	.0074	.0435	.0970
4.5	0.925	0.032	0.893	2.29	0.753	0.979	0.400	.0388	.0038	.0453	.0879
5.0	1.0	0.028	0.972	2.69	0.715	0.980	0.397	.0333	0	.0382	.0715
5.5	1.0	0.023	0.977	2.55	0.430	0.955	0.389	.0279	0	.0367	.0646

* Based on Ac

Half Axisymmetric Inlet Without Bypass

The external compression is the same for this inlet as the one discussed above. The overall contraction and internal contraction are also the same. The main difference is that there is no bypass duct and the initial cowl angle in flow aligned to avoid boundary layer separation. The internal lines, of course, are different (See Figure 3). The total capture area ratio is identical and the capture area ratio for the flow entering the combustor is higher (by 2 to 7 percent) since there is no bypass. The maximum inlet cowl radius is larger because of the flow aligned cowl. This necessitates reducing the cowl projected area (Ac) from 100.53 to 86.95 square inches. The net effect is less airflow entering the combustor. The total inlet drag coefficient is higher by approximately 40 percent or more. This is due to the higher cowl drag coefficient. The high cowl drag coefficient is due to the steeper cowl slope which causes a higher pressure coefficient (Cp) and greater projected area. The total pressure recovery (P_{T2}/P_{To}) and inlet exit Mach number (M_2) are approximately the same.

Performance estimates and inlet constants for the half axisymmetric inlet (without bypass) are presented in Table II. As in the case of the bypass inlet, bleed will probably be needed on the external compression surface and for the flow aligned inlet may be needed in the internal duct. Leading edges should be roughed to promote boundary layer transition.

Scoop Inlet

The scoop inlet has several advantages over other type inlets. The shock waves are weak and therefore less chance of boundary layer separation. The lines have low rates of curvature which helps to avoid separation and the cowl drag is approximately zero. The transition section between the inlet throat and combustor throat is simple (ellipse to a circle) which is less likely to separate and is easy to fabricate. The bypass flow can be readily dumped overboard at a low exit angle (low drag) or ducted to an air turbine. The leading edges are swept which reduces the bluntness requirements.

The disadvantages of the scoop inlet are the predictably of starting and the rather tedious aerodynamic design procedure. In the present design a low angle initial wedge is used to reduce the internal contraction required, thus helping inlet starting. The inviscid lines of the scoop inlet will produce a relatively large cut out on the bottom of the inlet. This cut out will aid inlet starting as air can spill overboard during the starting process. Two other features which facilitate inlet starting are the swept leading edges and the swept throat. A bypass duct will also be used which will be designed to aid inlet starting but minimize outflow after the inlet has started. The development of a scoop inlet for HYSAM application should include the experimental investigation of configuration variables (such as an alternate external wedge and bypass size).

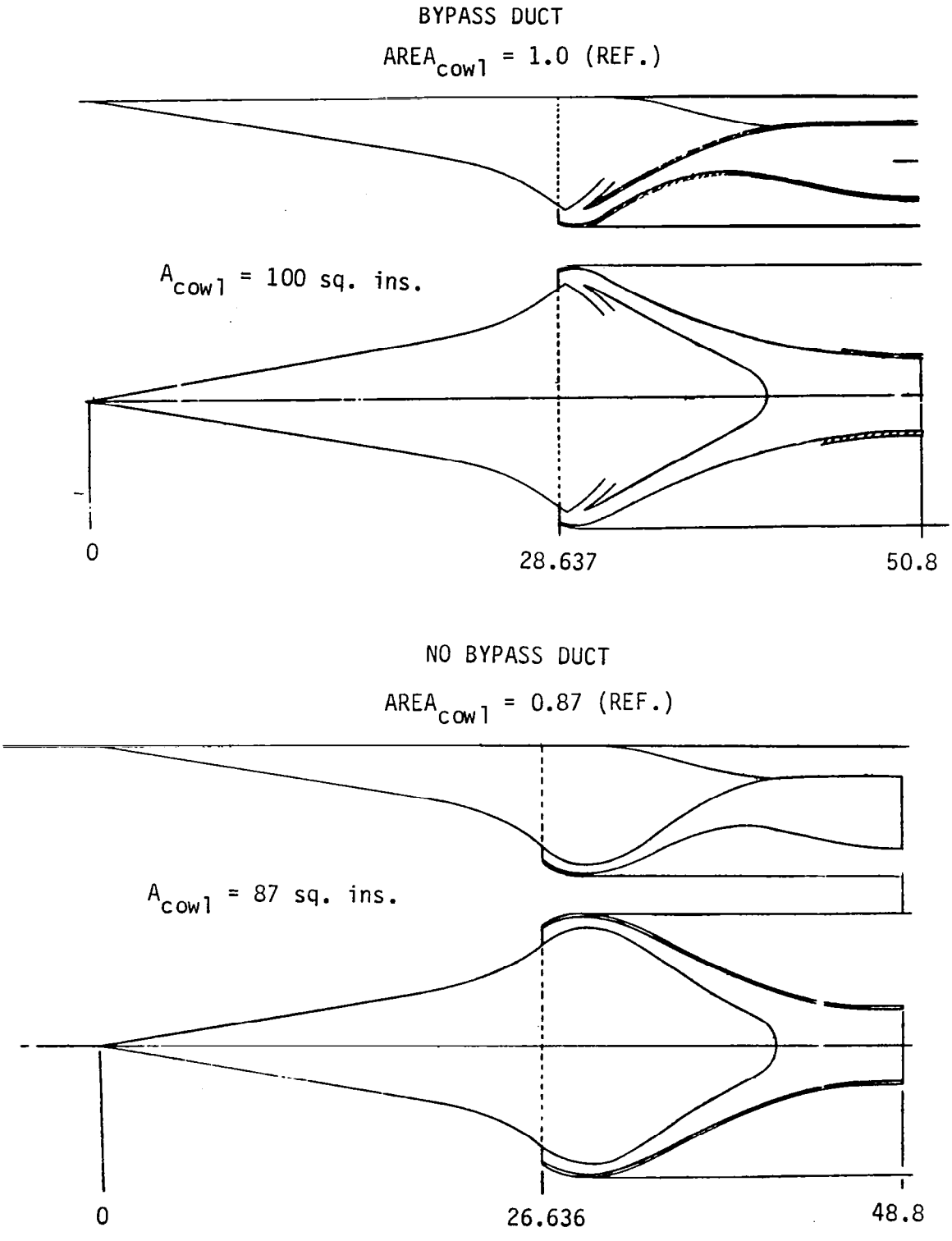

Figure 3. Half Axisymmetric Inlet Schematic with and without Bypass for Same Nacelle

TABLE II - Half Axisymmetric Inlet (without bypass)

External Compression - 10° half cone (blunted)
36° turning on spike
32.1° flow angle at cowl lip

Contraction - Overall, Ac/A_2 = 5.86
External, Ac/A_1 = 5.00
Internal, A_1/A_2 = 1.17

Areas - Ac = 86.95 sq. in. (Rc = 7.44 inches for half inlet)
A_1 = 17.39 sq. in.
A_2 = 14.85 sq. in (Equivalent diameter = 4.348)

Shock on cowl lip at Mo = 5, compression waves on cowl lip at Mo = 3.5

Cowl Lip - Blunted, flow aligned. External and internal angle = 32.1°

Mo	$\frac{Ao}{Ac}$	M_2	$\frac{P_{T2}}{P_{To}}$	KE2	C_{DA}*	C_{DC}*	C_{DT}*
3.0	0.740	1	0.920	0.987	.0151	.3881	.4032
3.5	0.795	1.67	0.896	0.987	.0113	.1428	.1541
4.0	0.857	2.06	0.828	0.983	.0074	.1256	.1330
4.5	0.925	2.38	0.769	0.981	.0038	.1340	.1378
5.0	1.0	2.65	0.713	0.980	0	.1192	.1192
5.5	1.0	2.53	0.429	0.955	0	.1062	.1062

* Based on Ac

TABLE II - CONT.

Coordinates - High Compression, Convention Inlet

Spike

x	y	θ	
18.165	3.203	10°	St Line
20.074	3.574	10°	
21.983	4.010		
23.891	4.709		
25.800	5.867	36°	St Line
27.071	6.791	36°	

Centerbody

x	y	θ
27.071	6.790	36°
27.675	7.169	27.441°
28.278	7.425	18°
28.854	7.549	6°
29.682	7.595	0.29°
30.511	7.569	-3.9°

Cowl - Internal

x	y	θ	
26.636	7.441	32.1°	
27.682	7.960	20.1°	
28.614	8.200	8.86°	
29.545	8.237	-3.9°	St Line
30.552	8.168	-3.9°	

Scoop type inlets were previously developed by TMC on the PLUTO program in the 1960's. These inlets operated at Mach numbers in the vicinity of three (3). A analytical technique was developed that permitted determining the contours and flow properties at the design Mach number. The method was not theoretically exact but agreement between experimental data and predictions were excellent. The method requires a plane of symmetry and that the projected throat shape be inside the projected capture shape as shown below.

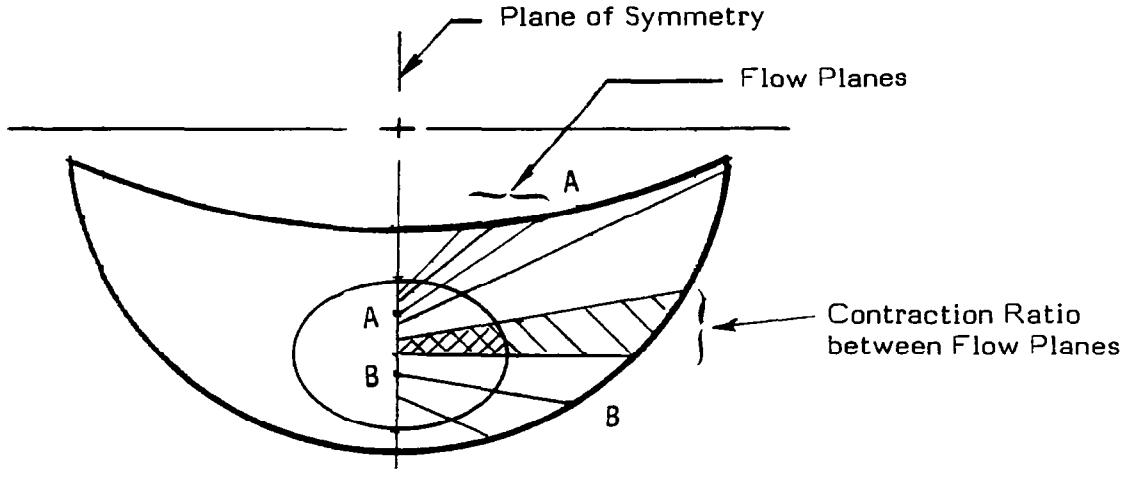

The ratio of the projected initial area between flow planes to the projected throat area between flow planes must equal the contraction ratio between the initial projected area and the throat area. Flow planes cannot cross. The axial Mach number distribution along all flow planes in the plane of symmetric must be identical as indicated below (i.e., along L).

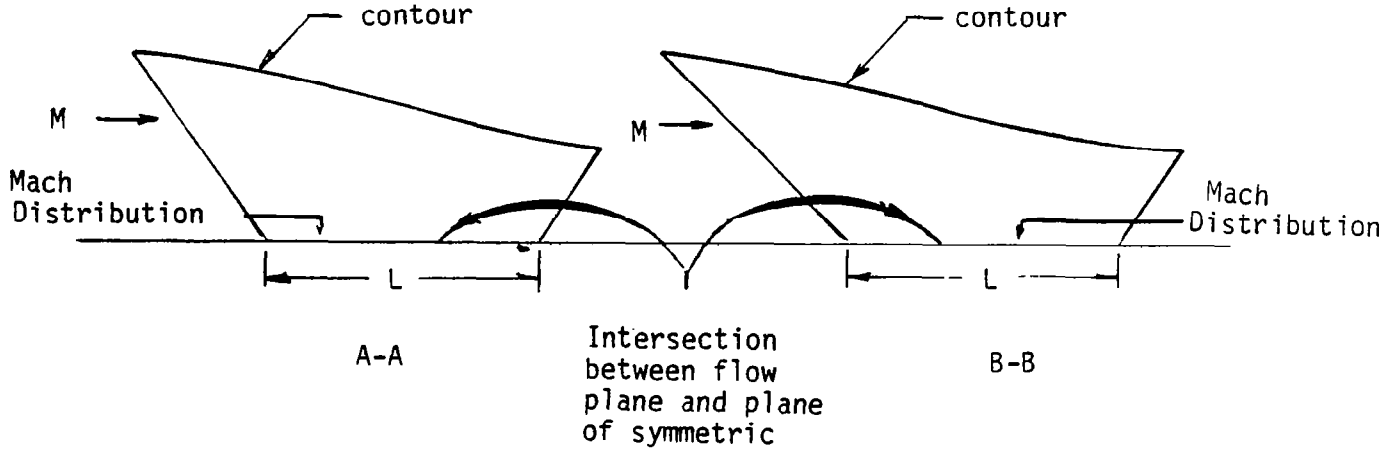

The flow in each flow plane is axisymmetric; however, the lines along which the Mach number distribution is constant are lines on cylinders in axisymmetric flow such the the contraction ratio is satisfied in each flow plane.

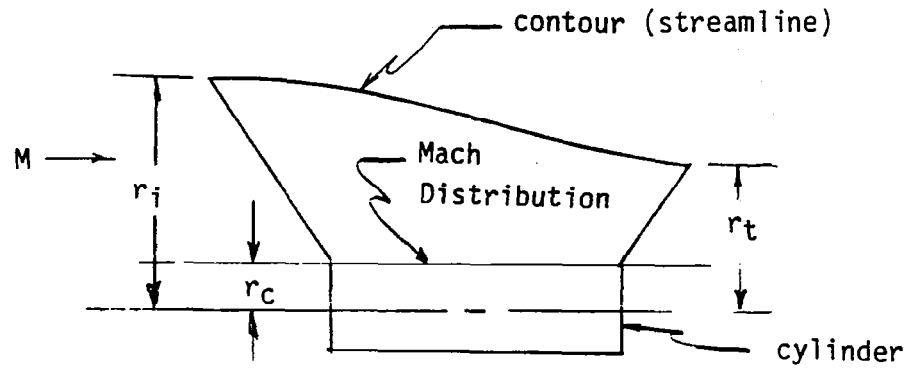

where $\frac{r_i^2 - r_c^2}{r_t^2 - r_c^2}$ = C.R.

The method of characteristics is used to determine the flow field in each flow plane. Streamlines are traced to determine the contour.

The scoop inlet proposed for the WADM application has been partially designed (to the extent that feasibility of design was established). The concept is shown in Figure 4. The external wedge is 5 degrees and will probably have a platypus shaped leading edge (matching the external and internal contours will determine the wedge leading edge shape; this is the last step in the design procedure). The capture shape is a combination of a circular segment and a rectangle as shown in Figures 4 and 5. This shape will fit into the launch tube and give a higher projected cowl area then the axisymmetric designs (118.7 square inches compared to 100.5 square inches). The throat is an ellipse with semiaxes as shown in Figure 5. The cross-hatched area is the initial wedge. The non cross-hatched area is a shape that has to be determined by the method previously discussed. However, it has been established that the initial shape and the throat shape are compatible with the scoop design method.

Inlet constants and performance are presented in Table III, The performance at the present point in the design is largely a estimate. When the aerodynamic lines are completed, better performance estimates can be made.

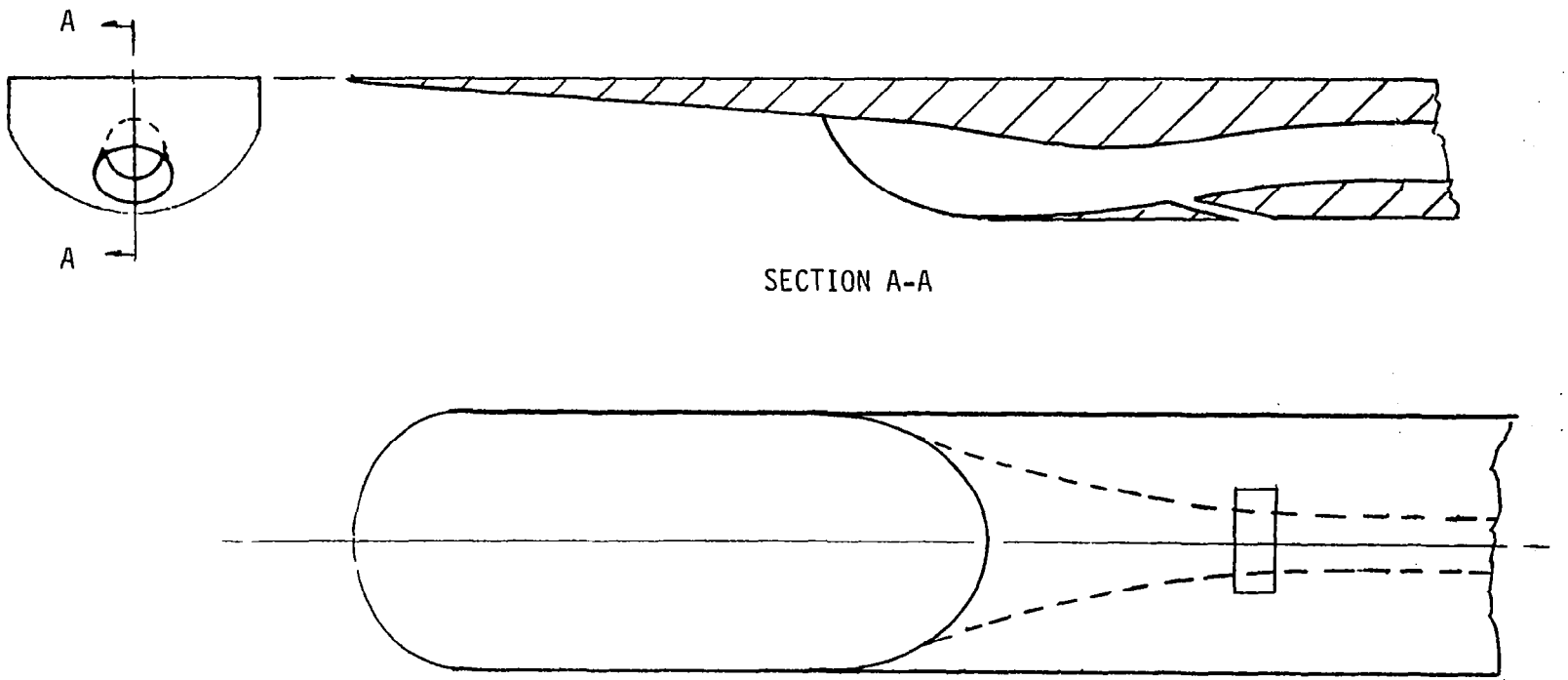

Figure 4. Scoop Inlet Schematic

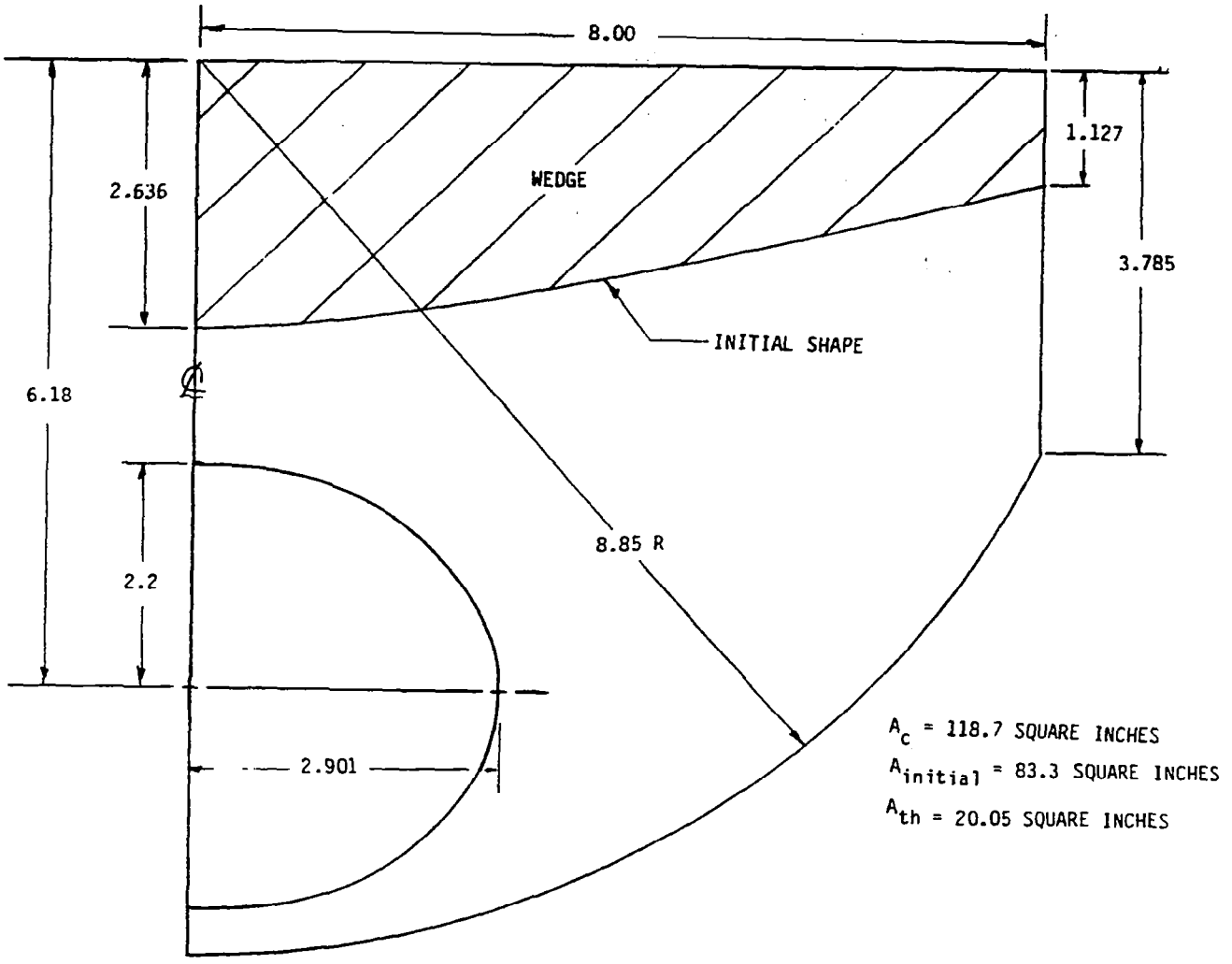

Figure 5. Scoop Inlet Geometry

TABLE III - Scoop Inlet

External Compresion - 5° wedge

Contraction -	Overall	5.92
	External	TBD
	Mixed	TBD
	Internal	TBD

Areas - Ac = 118.7 sq. in.
At = 20.05 sq. in. (Equivalent Diameter 5.053)

Design Mach Number 4.5

Estimated Performance*

Mo	$\frac{Ao}{Ac_T}$	M_2	$\frac{P_{T2}}{P_{To}}$	C_{DC}
3.0	.74		.92	0
3.5	.83		.90	0
4.0	.92		.83	0
4.5	1.0	2.3	.77	0
5.0	1.0		.71	0
5.5	1.0		.64	0

REFERENCES

1. Hunt, J. L., Lawing, P. L., Marcum, D. C. and Cubbage, J. M., "Conceptual Study of Hypersonic Airbreathing Missiles," AIAA Paper No. 78-6, Huntsville, Alabama, January 16-18, 1978.

2. Hunt, James L., Johnston, Patrick J., Cubbage, James M., and Marcum, Don C., Jr., and Carlson, Charles H., "A Mach 6 Airbreathing Surface-to-Air Missile (HYSAM). 1980 JANNAF Propulsion Meeting - Volume II, Karen L. Strange, ed., CPIA Publ. 315 (Contract N00024-78-C-5384), Appl. Phys. Lab., Johns Hopkins Univ., Mar. 1980, pp. 321-385.

3. Burnette, T., "Dual Mode Scramjet - Part III - Engine Design and Performance Characteristics", The Marquardt Company, AFAPL-TR-67-132, Part III, April 1968.

4. Heins, A. E., Jr., Reed, G. J., and Woodgrift, K. E., "Hydrocarbon Scramjet Feasibility Program, Part III. Free Jet Engine Design and Performance," AFAPL-TR-70-74, Part III, Jan. 1971.

5. A. L. Baer, "Wind Tunnel Tests of a Marquardt Dual Mode Scramjet Inlet Model at Mach Numbers from 2 to 10", AEDC-TR-67-105, July 1967.

6. Carlson, Charles H., "Scramjet Performance Parametrics for Hypersonic Airbreathing Missile Application", NASA CR 3575, 1982.

1. Report No.	2. Government Accession No.	3. Recipient's Catalog No.
NASA CR-3742		

4. Title and Subtitle	5. Report Date
PRELIMINARY SCRAMJET DESIGN FOR HYPERSONIC AIRBREATHING MISSILE APPLICATION	November 1983
	6. Performing Organization Code
7. Author(s)	8. Performing Organization Report No.
Charles H. Carlson	S-1585
	10. Work Unit No.
9. Performing Organization Name and Address	11. Contract or Grant No.
The Marquardt Company 16555 Saticoy Street Van Nuys, California 91409	NAS1-15434
	13. Type of Report and Period Covered
12. Sponsoring Agency Name and Address	Contractor Report
National Aeronautics and Space Administration Washington, D.C. 20546	14. Sponsoring Agency Code

15. Supplementary Notes

Langley Technical Monitor: James L. Hunt
Final Report

16. Abstract

A conceptual design study of a scramjet engine was conducted for a hypersonic surface to air missile (HYSAM). The definition of the engine was based upon the requirements of accelerating the HYSAM from Mach 4 at 20,000 feet to Mach 6 at 100,000 feet and the cruise conditions at Mach 6. The resulting external and internal environmental conditions were used by various engineering disciplines performing design, stress and heat transfer analysis. A detailed structural analysis was conducted along with an indepth thermal analysis. Structurally all the components within the system exhibit positive margins of safety. A feasible concept was defined which uses state-of-the-art materials and existing TMC technology. The engine basically consists of a three-dimensional carbon/carbon combustor/nozzle secured to an FS-85 columbium inlet. The carbon/carbon liner is sheathed with carbon felt insulation to thermally protect the FS-85 structure and skin. The thermal analysis of the engine indicates that a thermally viable configuration exists.

17. Key Words (Suggested by Author(s))	18. Distribution Statement
Scramjet HYSAM Carbon/Carbon FS-85 Columbium	Unclassified - Unlimited Subject Category 07

19. Security Classif. (of this report)	20. Security Classif. (of this page)	21. No. of Pages	22. Price
Unclassified	Unclassified	68	A04

N-305

For sale by the National Technical Information Service, Springfield, Virginia 22161